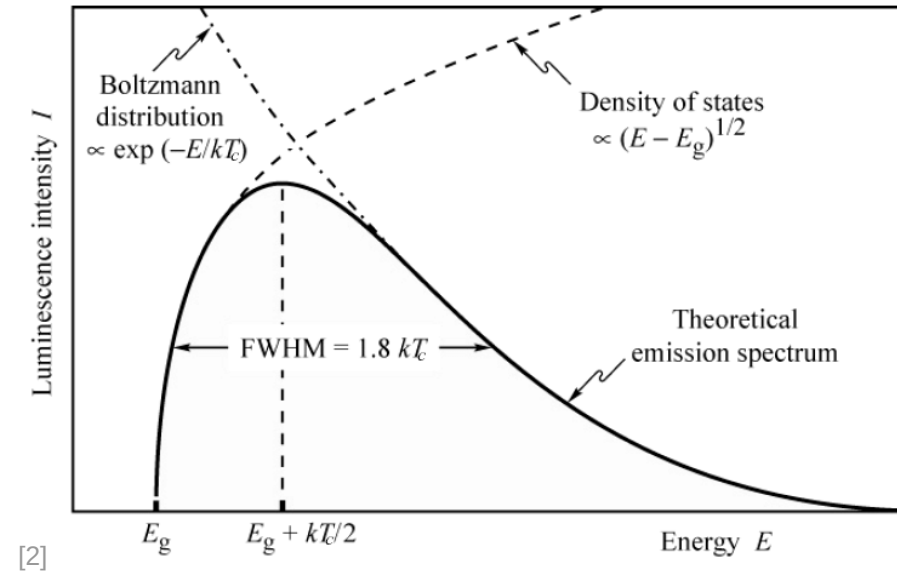
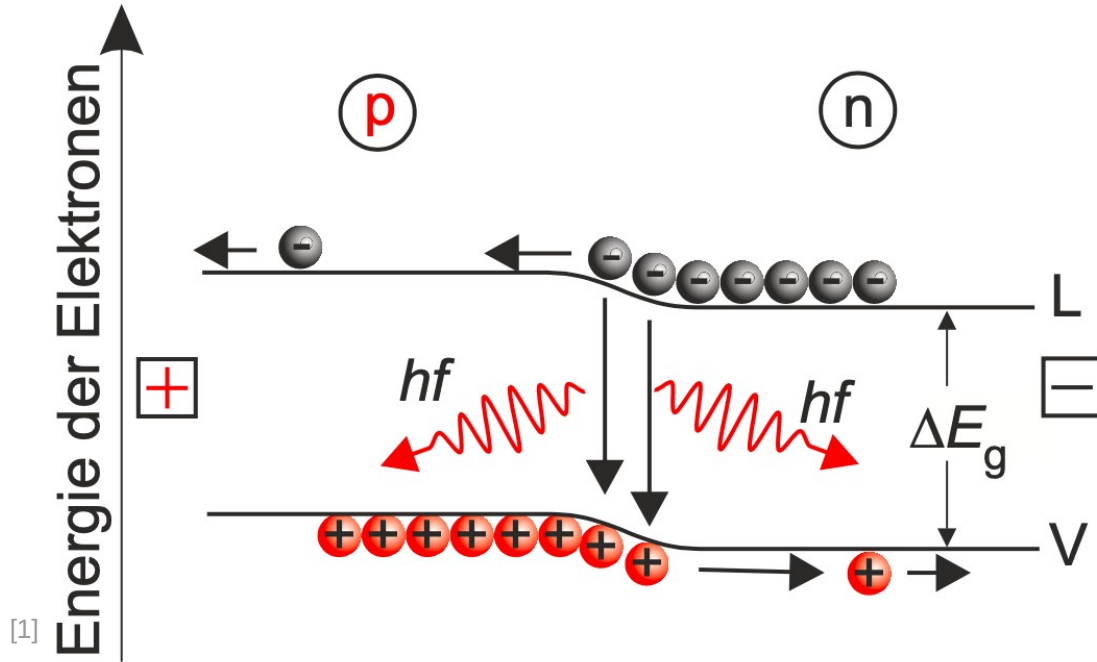


**Threshold and gain measurements of AlGaN-
based UVC lasers
&
Temperature dependent electroluminescence
spectroscopy on AlGaN-based 235nm far-UVC
LEDs with different active region growth
temperatures**

Schwellen- und Gewinnmessungen bei AlGaN- basierten UVC Lasern & Temperaturabhängige Elektrolumineszenz- spektroskopie an 235 nm AlGaN UVC LEDs mit variabler Wachstumstemperatur der aktiven Zone

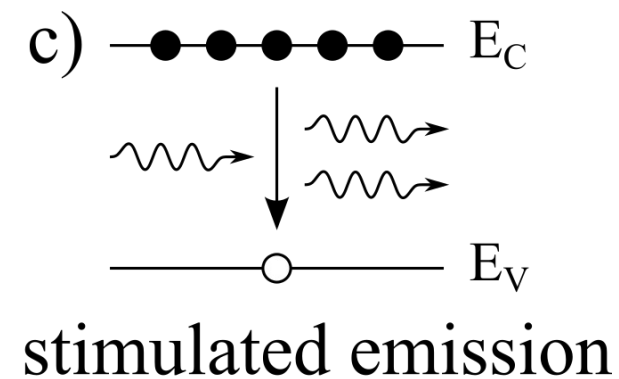
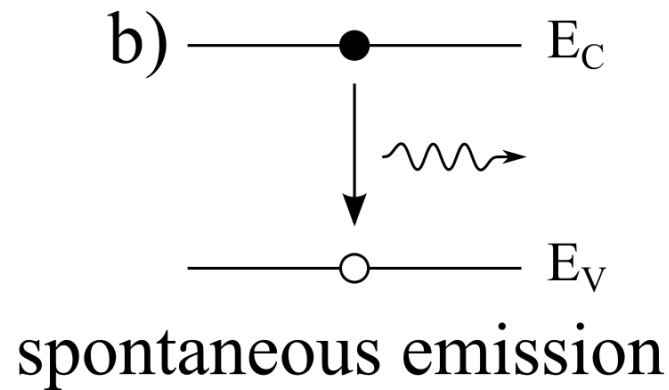
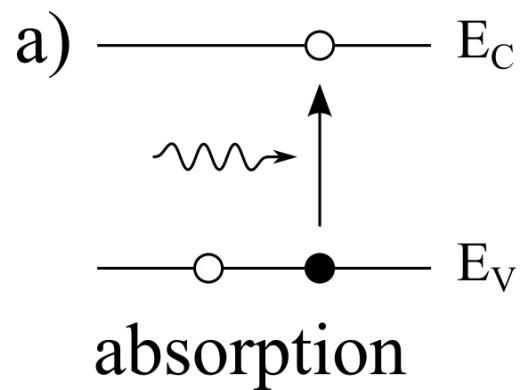
LED Bändermodell



[1] *Das Neue Physikalische Grundpraktikum*, Eichler, Kronfeldt, Sahn

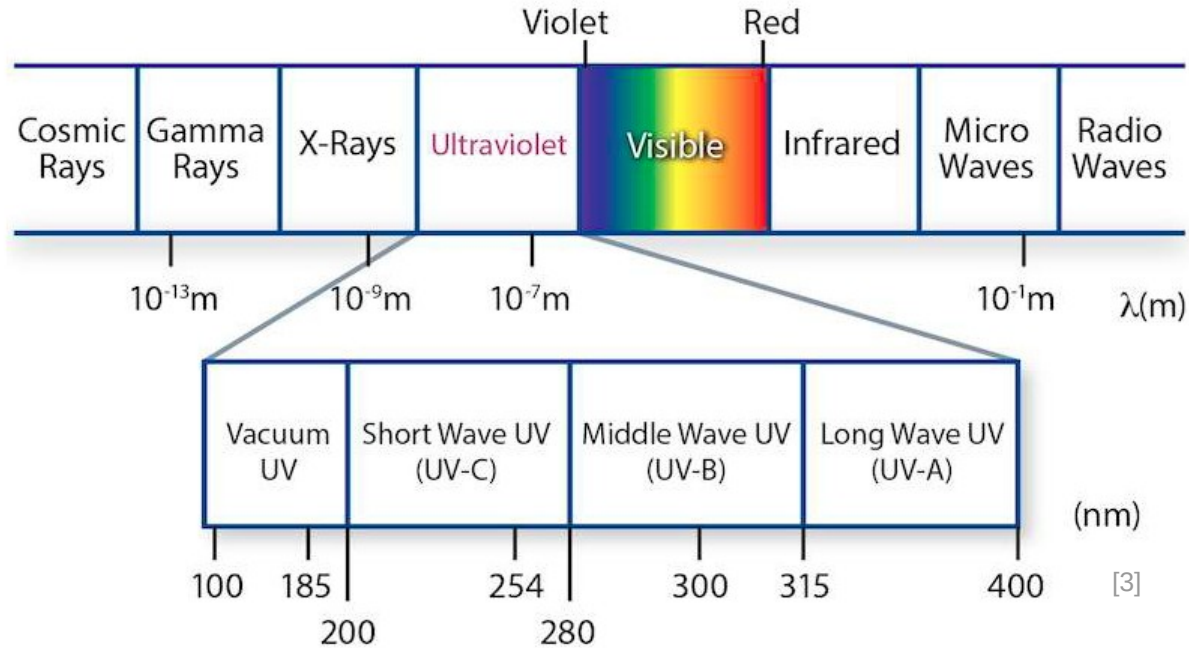
[2] https://www.researchgate.net/figure/Theoretical-light-emitting-diode-spectrum-as-a-product-of-the-density-of-energy-states_fig34_268054048

Photon-Elektron-Wechselwirkung



[1]

UV-Spektrum



UV-C Anwendungen



LASIK eye surgery...

HOW IT WORKS

Cornea
Once tissue has been removed, the flap is folded back onto the cornea and heals quickly.

UV laser
Pulses of ultraviolet laser light vaporise surface tissue, reshaping the cornea.

Bull's-eye
A laser projects a target on the eye at which the UV laser beam can aim.

Flap
A special surgical knife slices a flap open on the surface of the cornea.

Retina
After surgery, light rays entering the eye are focused to a point on the retina, producing a much clearer image.

DID YOU KNOW?
LASIK is a kind of refractive laser eye surgery used to treat near- and far-sightedness and astigmatism.

[4] <https://www.coherent.com/de/lasers/excimer/indystar>

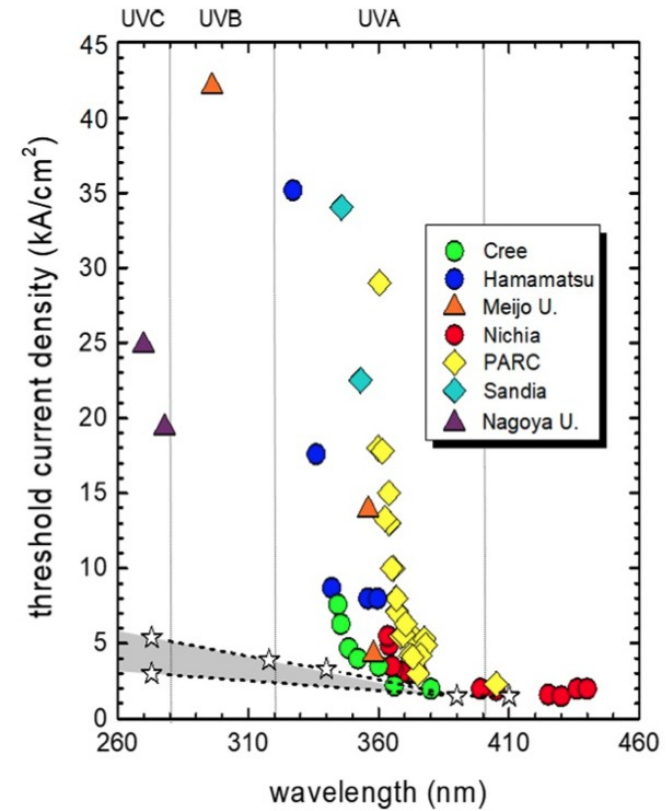
[5] <https://www.kotte-zeller.de/origin-outdoors-trinkflasche-fairbanks-mit-uv-wasserfilter-schwarz-fuer-outdoor-zur-notversorgung>

[6] <https://www.howitworksdaily.com/how-does-laser-eye-surgery-work/>

Motivation



[7]

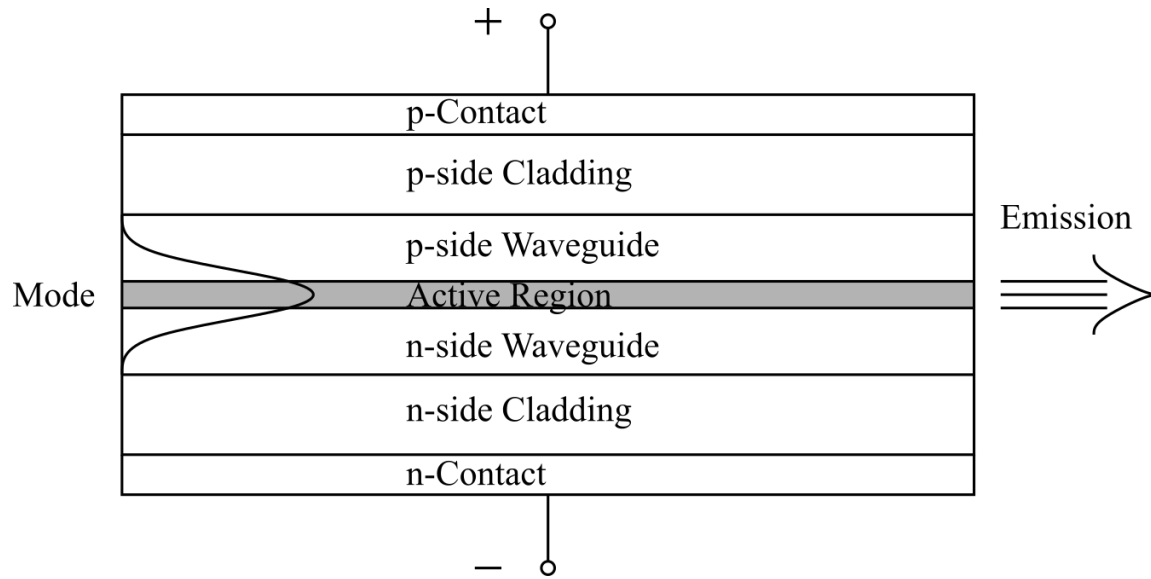


[8]

[7] <https://www.coherent.com/de/lasers/excimer/indystar>

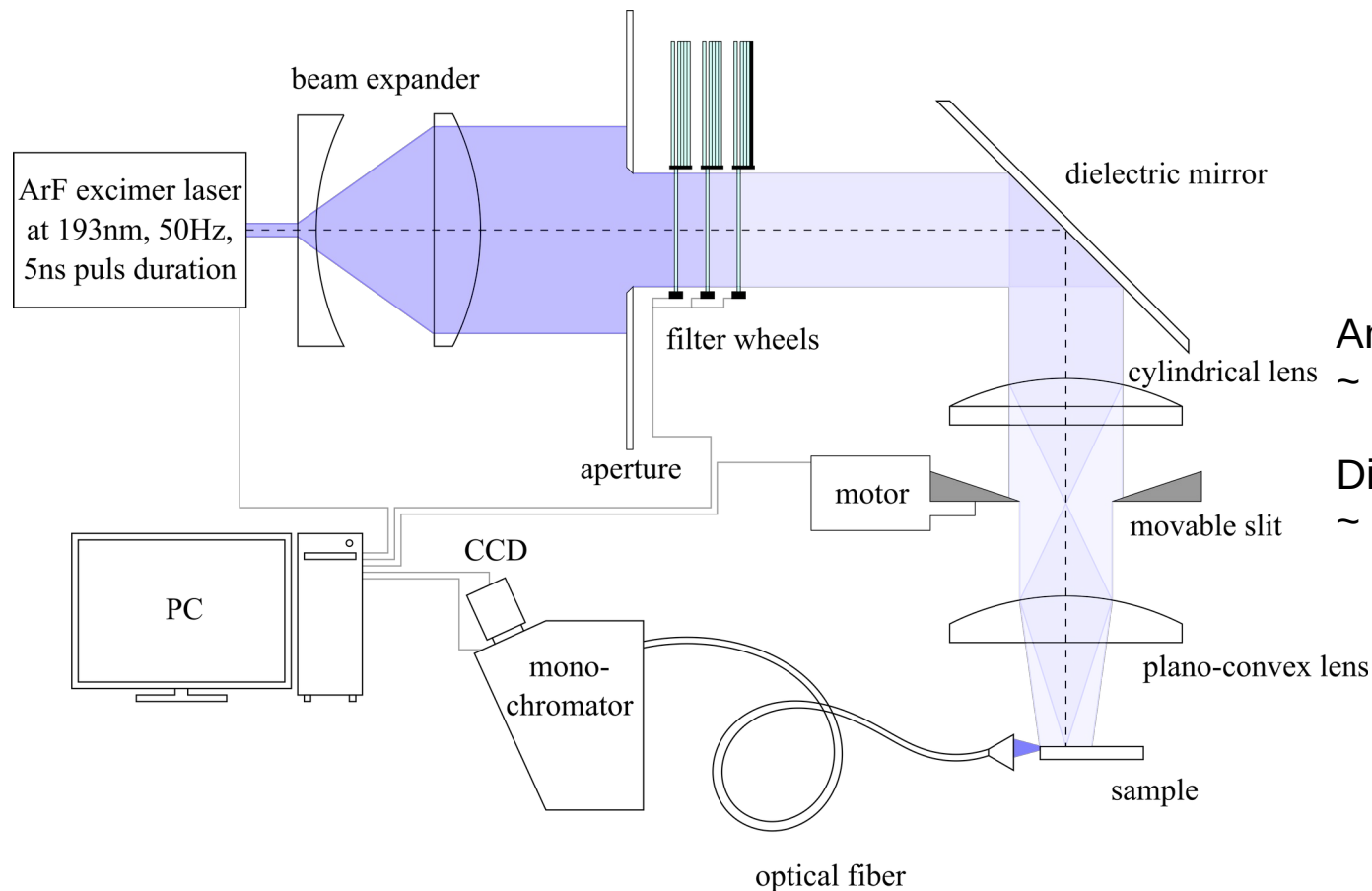
[8] Amano et. al. (2020) J. Appl. Phys., 53,503001

Edge-Emitting Lasers (EELs)



AlN 10 nm cap
$Al_{0.63}Ga_{0.37}N$ 50 nm p-WG
$Al_xGa_{1-x}N$ y nm SQW
$Al_{0.63}Ga_{0.37}N:Si$ 50 nm n-WG
$Al_{0.76}Ga_{0.24}N:Si$ 900 nm cladding
$Al_{0.76}Ga_{0.24}N$ 100 nm buffer
AlN- $Al_{0.76}Ga_{0.24}N$ 25 nm buffer
HTA/ELO AlN/sapphire substr.

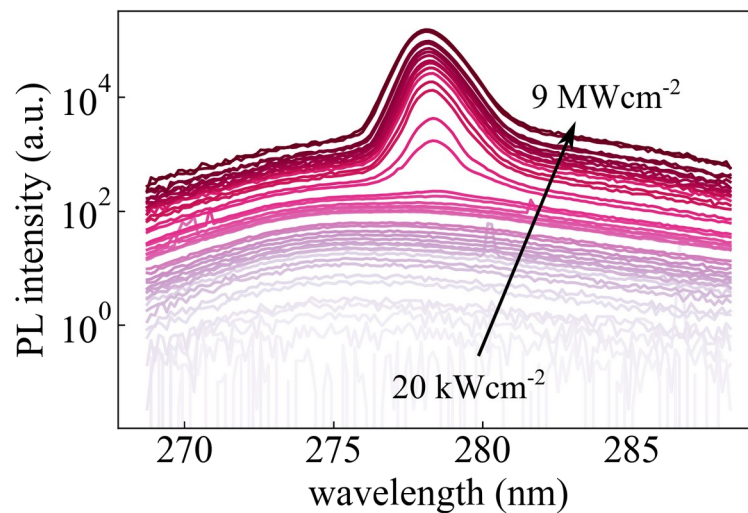
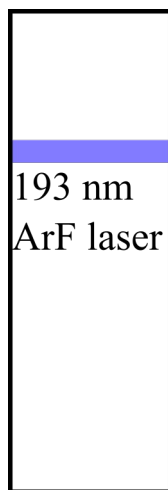
Photolumineszenzaufbau



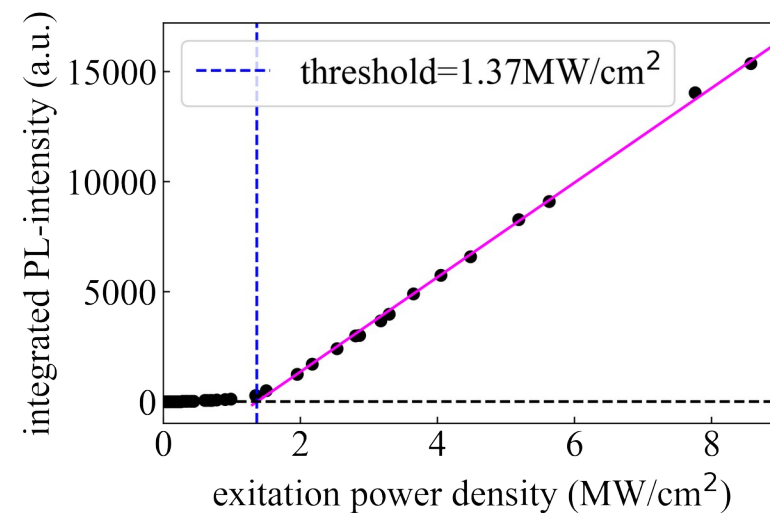
Anregungsleistungsdichte:
~ 30 kWcm⁻² - 9 MWcm⁻²

Dimensionen des Leuchtstreifens:
~ 14 μm × (50 - 500) μm

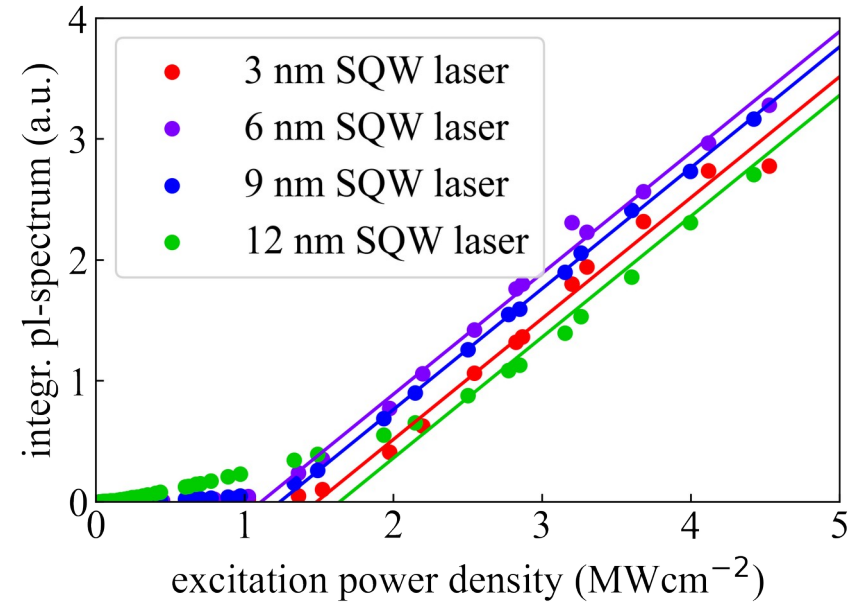
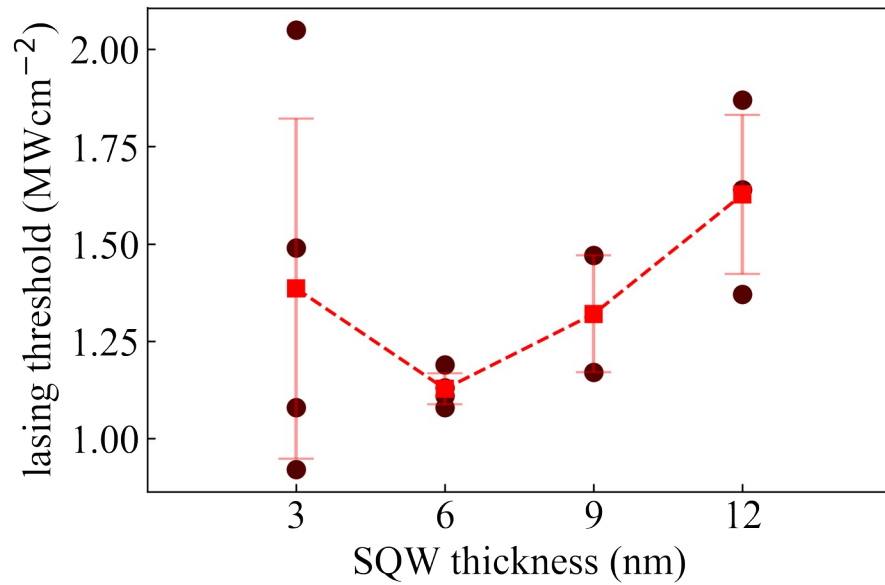
Messung und Berechnung der Schwelle



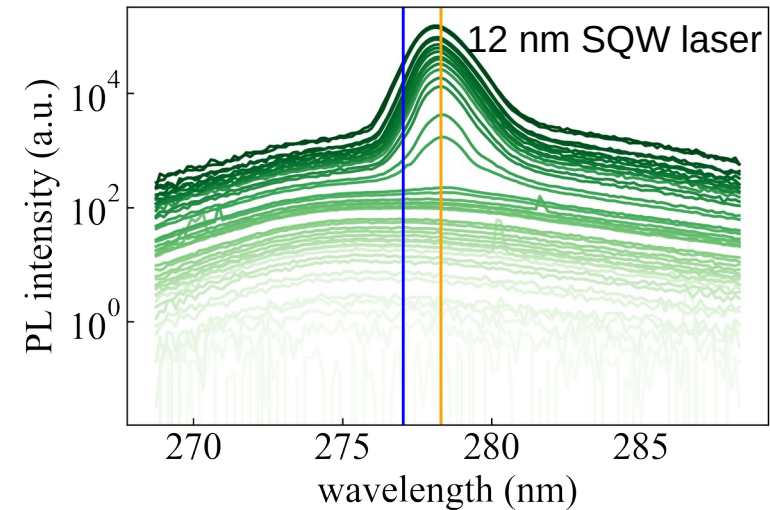
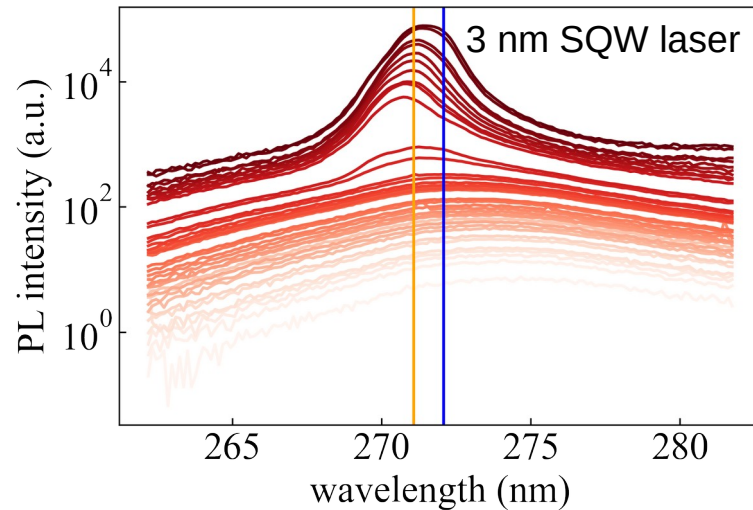
12 nm SQW laser (TS5862)



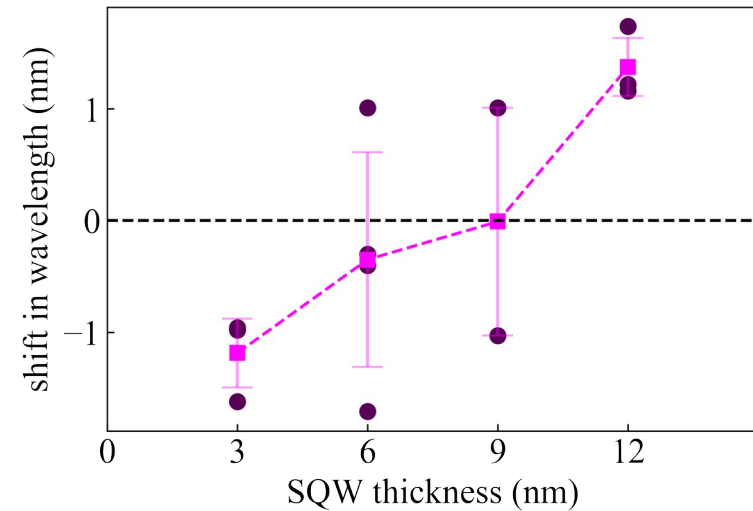
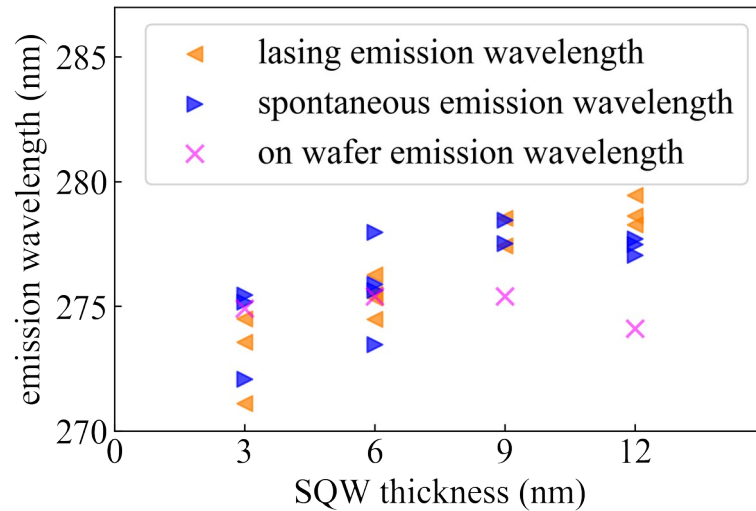
Laserschwelle



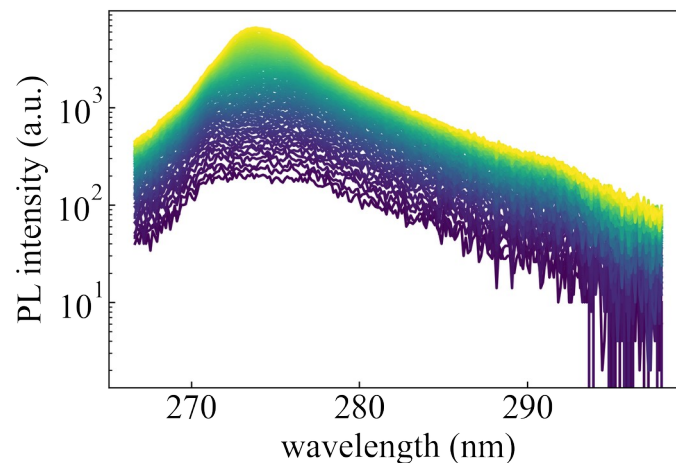
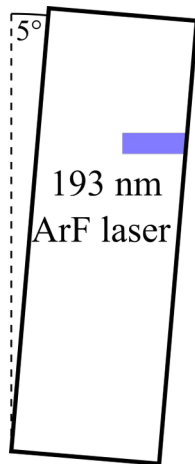
Emissionsspektren von AlGaN basierten optisch angeregten Lasern



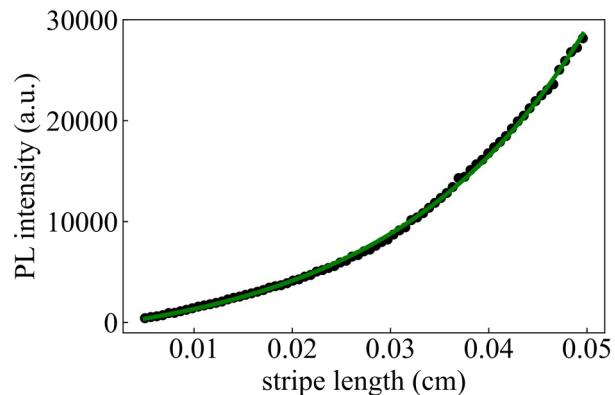
Emissionswellenlänge



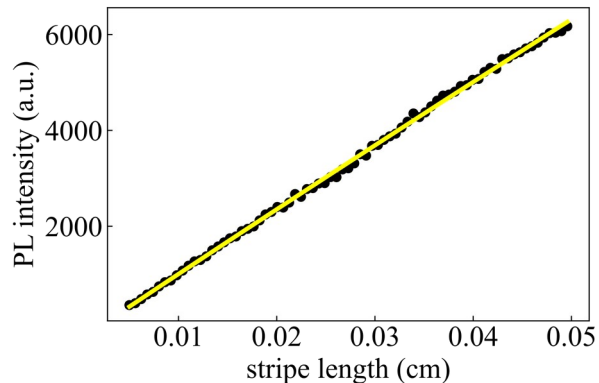
Gewinnmessung und Berechnung



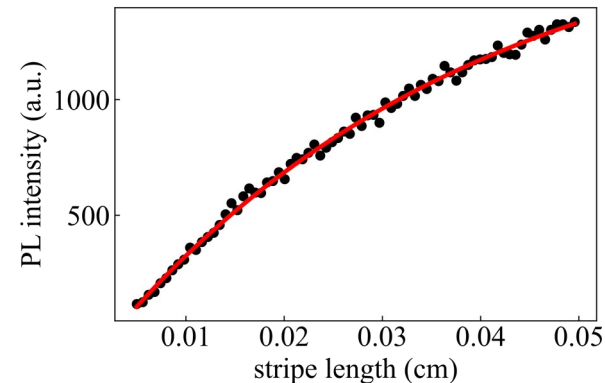
a) positive gain (276 nm)



b) zero gain (280 nm)

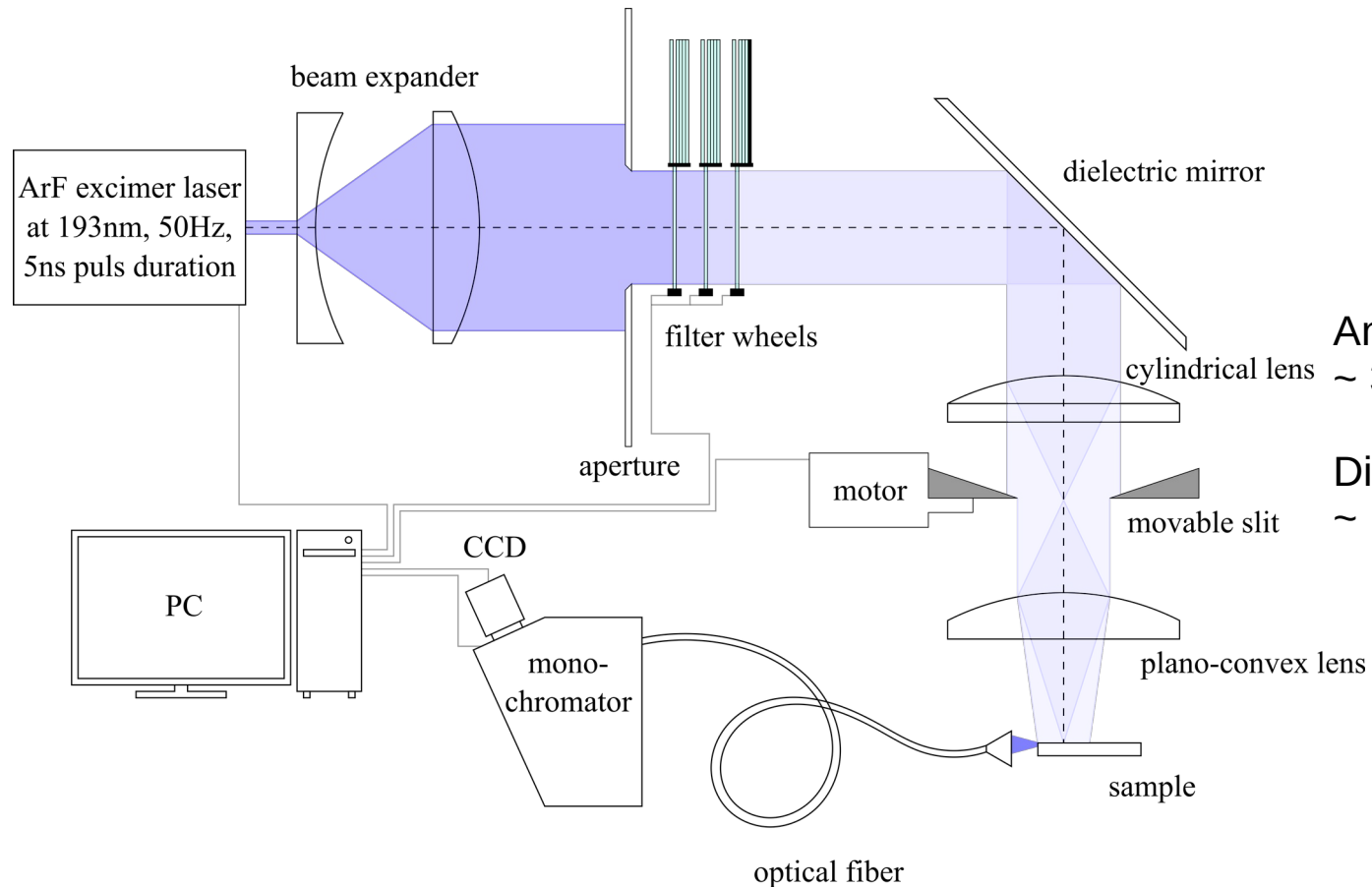


c) negative gain (269 nm)



6 nm SQW laser (TS5858)

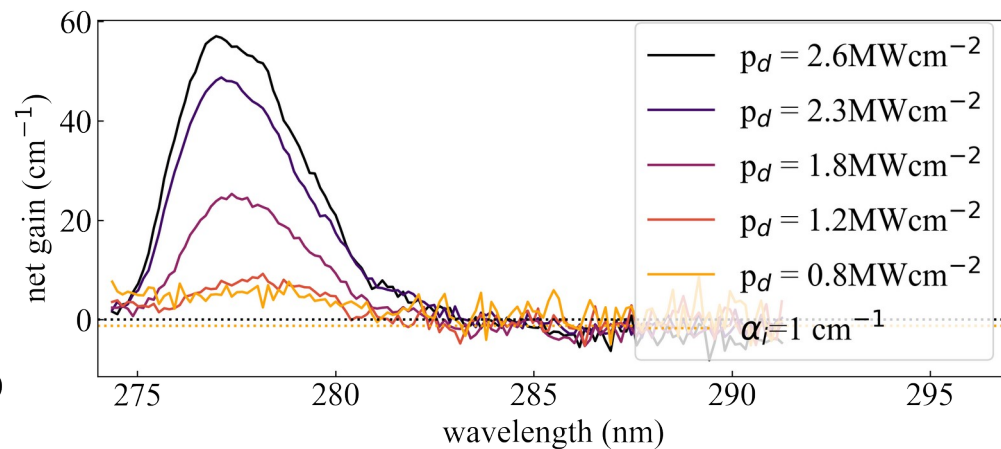
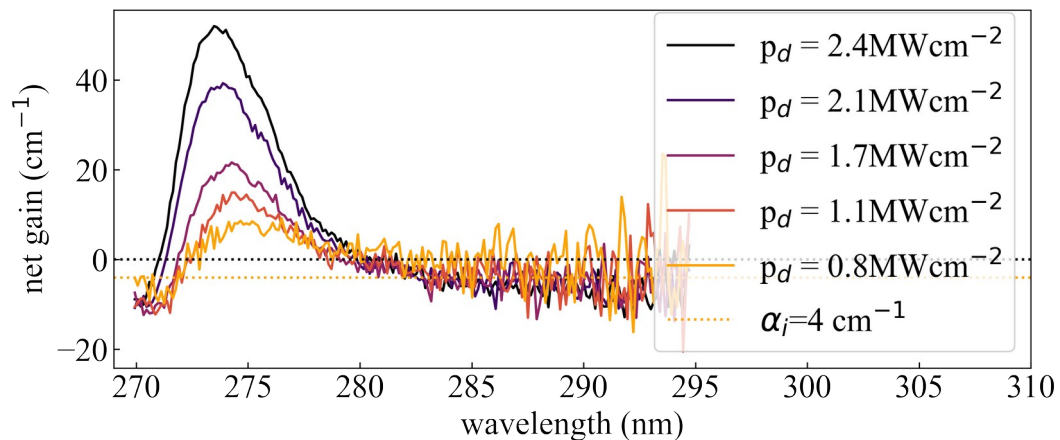
Photolumineszenzaufbau



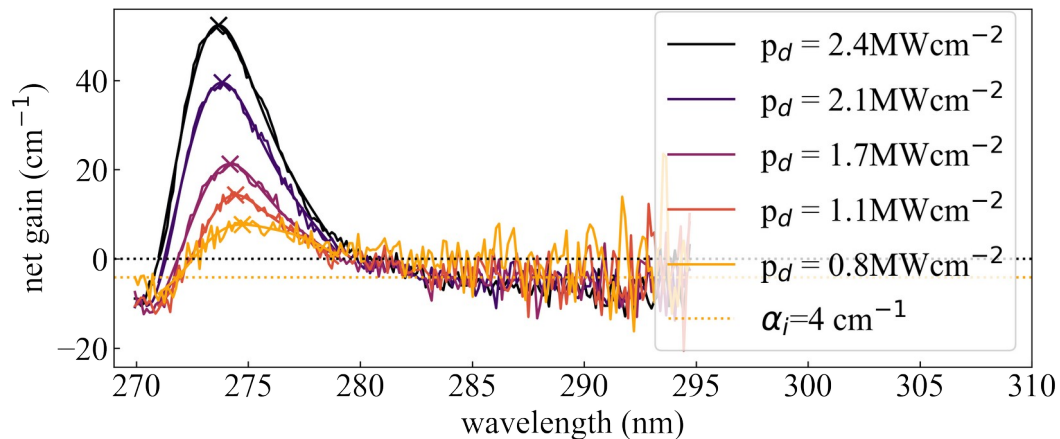
Anregungsleistungsdichte:
~ 30 kWcm⁻² - 9 MWcm⁻²

Dimensionen des Leuchtstreifens:
~ 14 μm × (50 - 500) μm

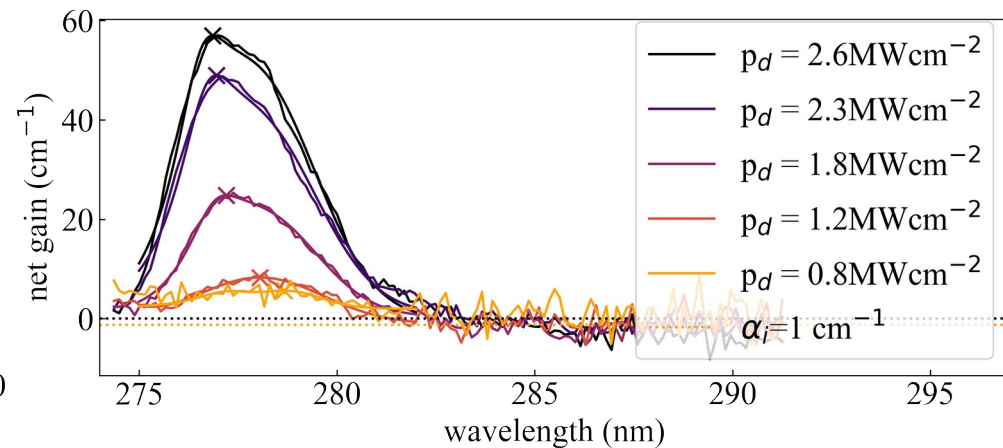
Gewinnspektren



Gewinnspektren

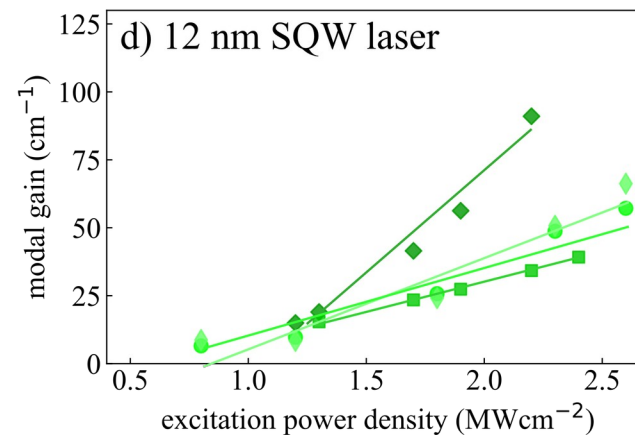
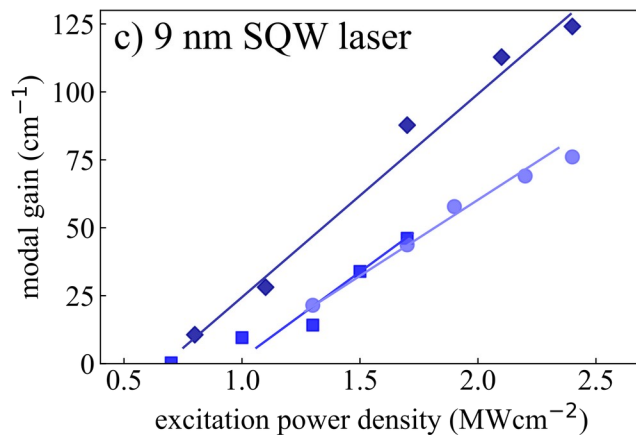
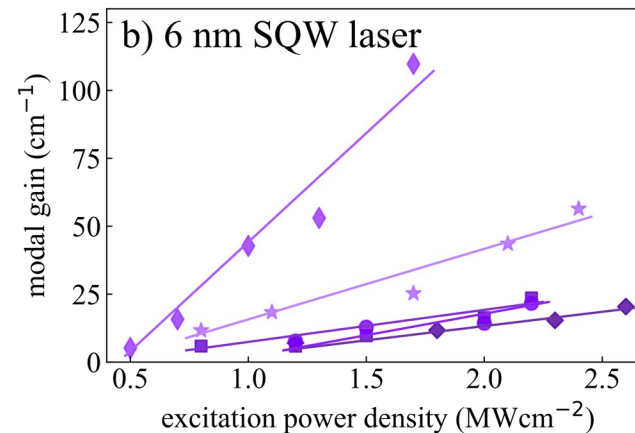
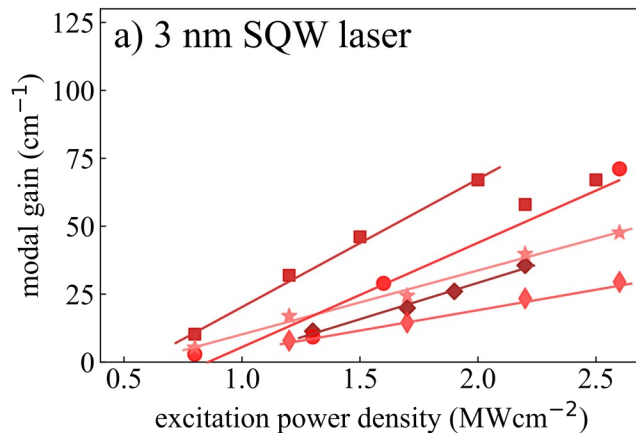


6 nm SQW laser

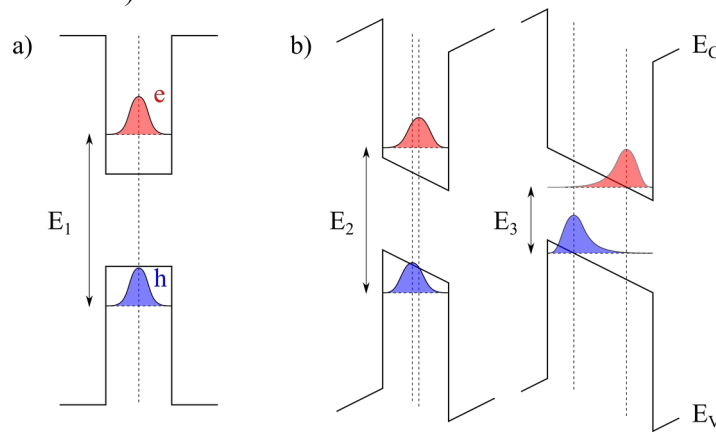
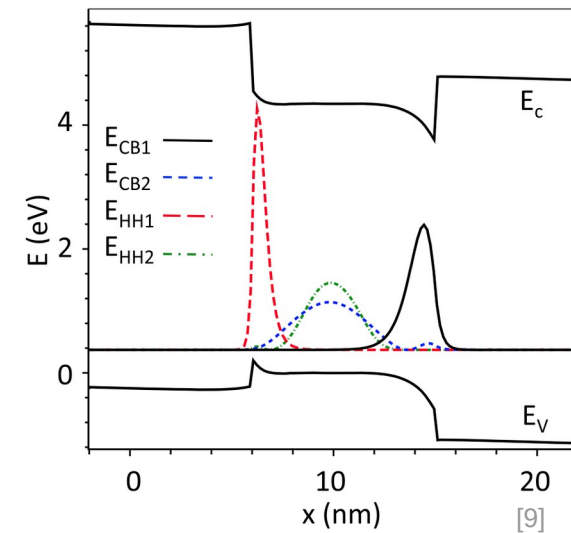
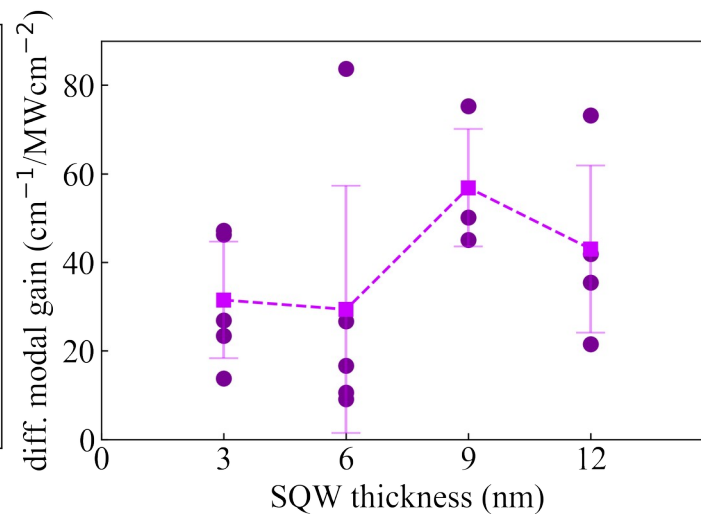
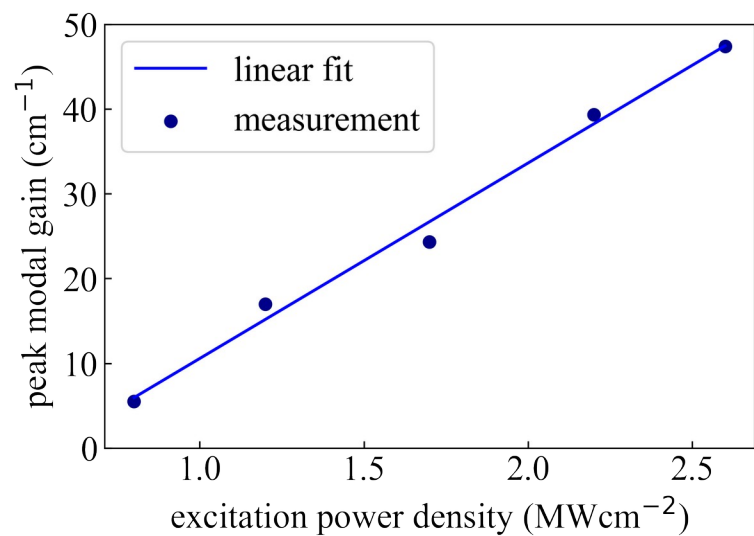


12 nm SQW laser

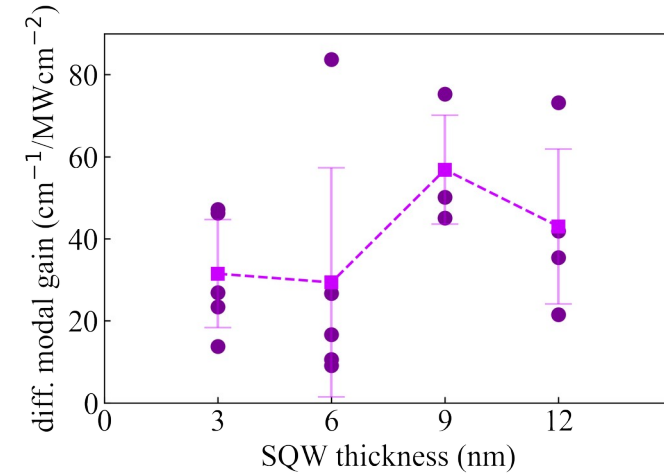
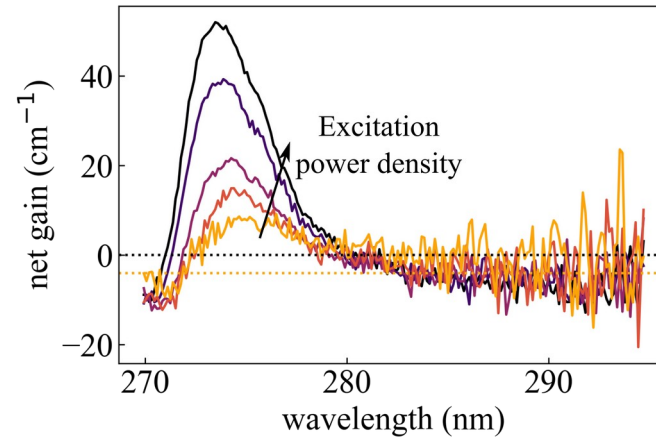
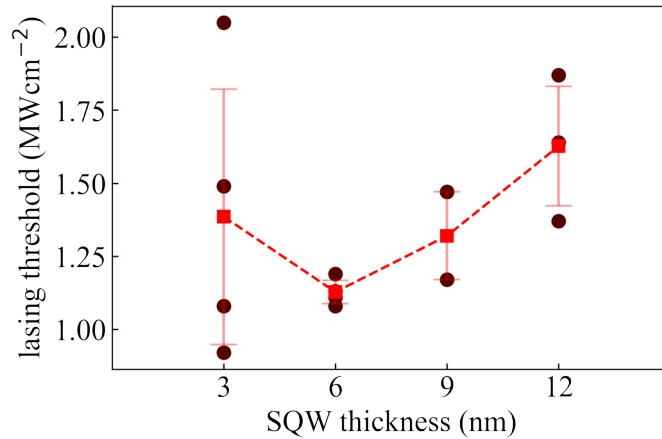
Modaler Gewinn



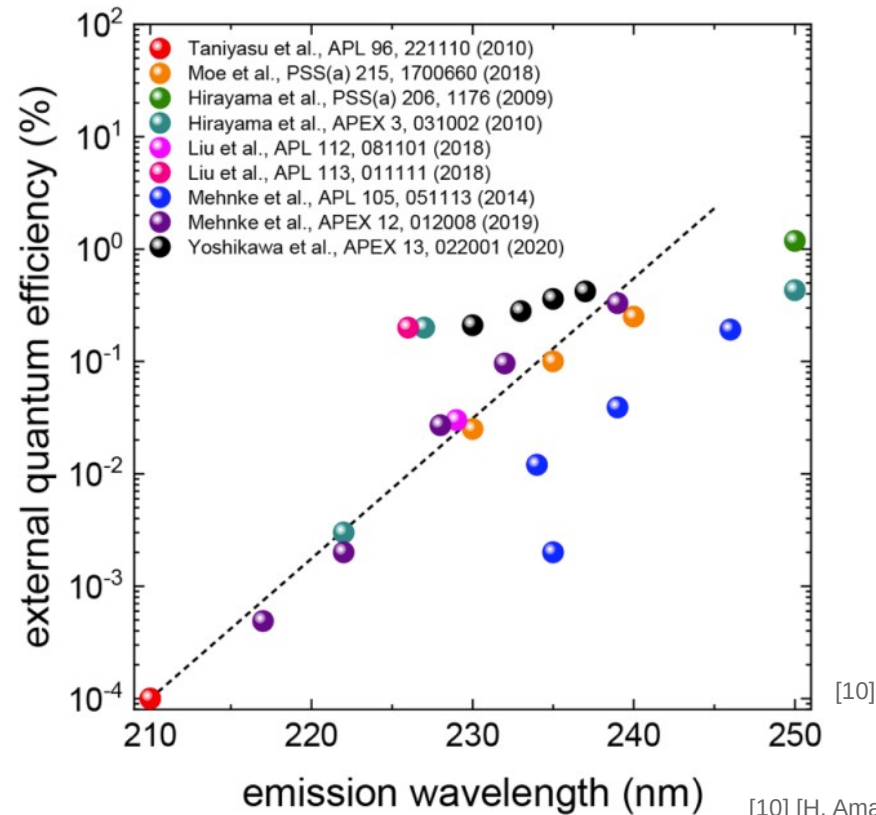
Differentieller Gewinn



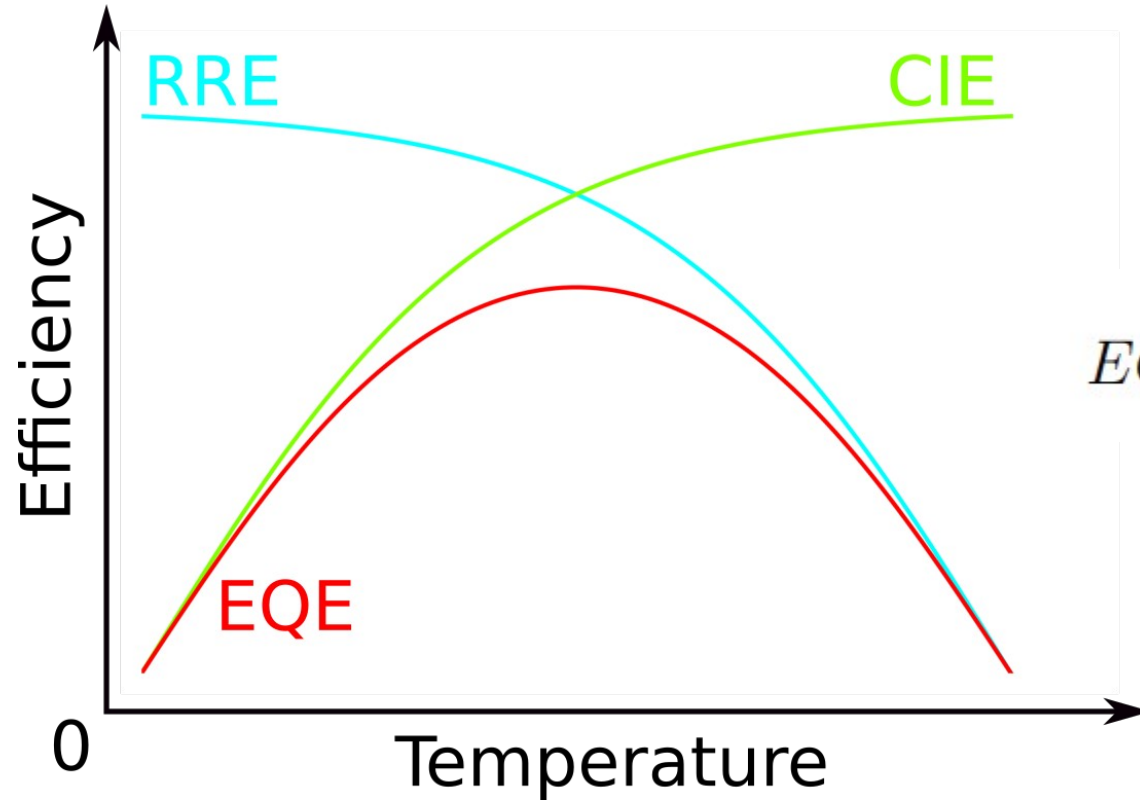
Zusammenfassung und Ausblick



Motivation

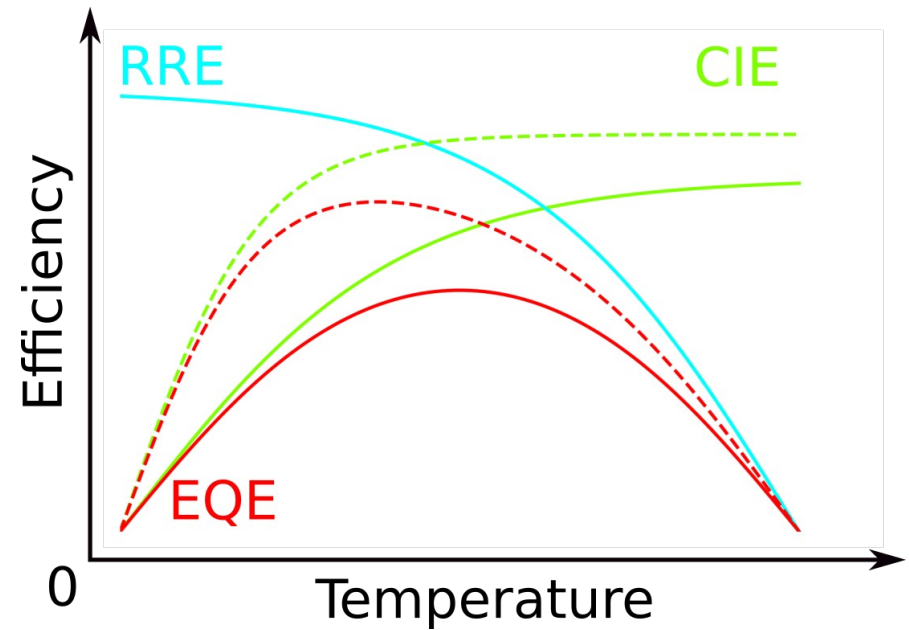
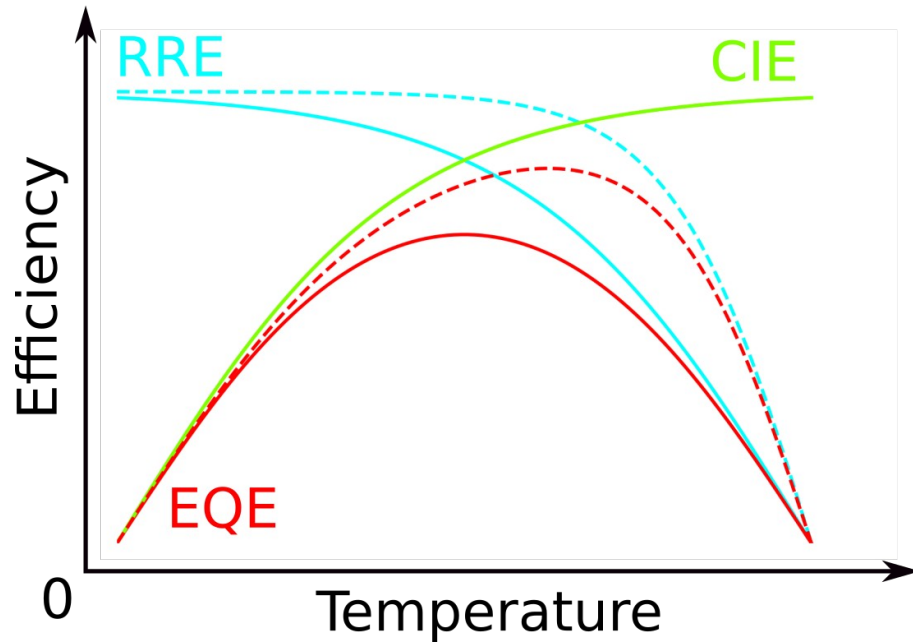


Externe Quanteneffizienz (EQE)

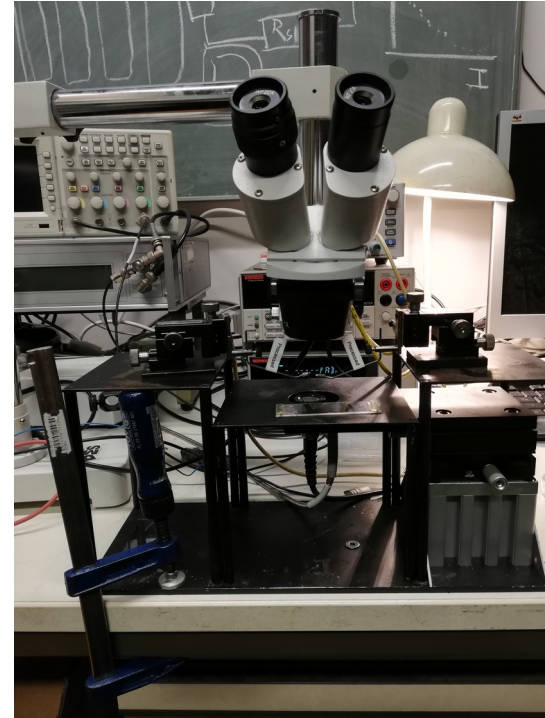
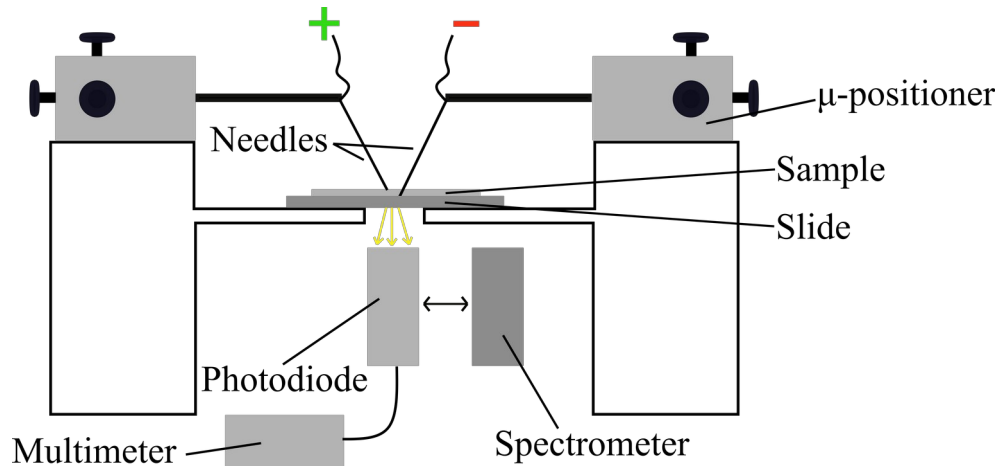


$$EQE = LEE \cdot CIE \cdot RRE$$

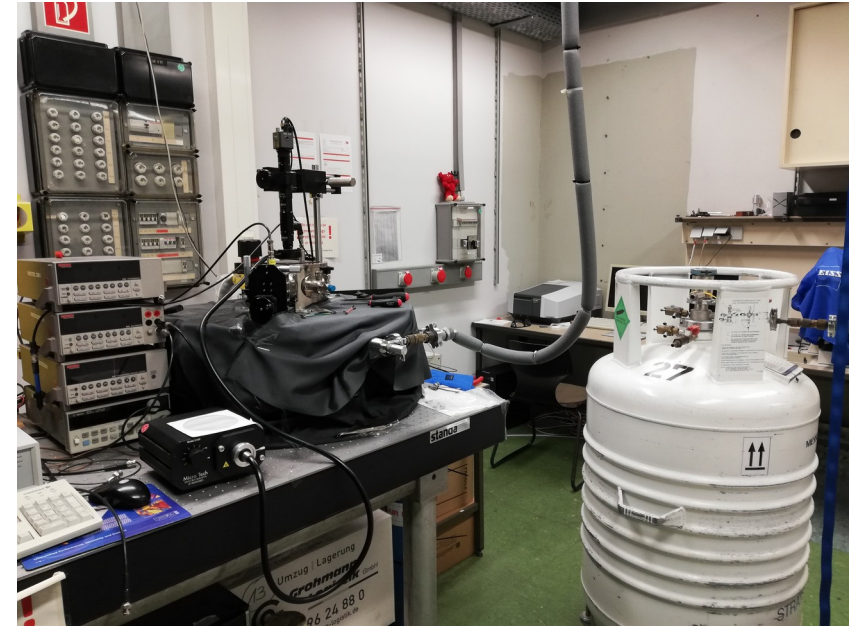
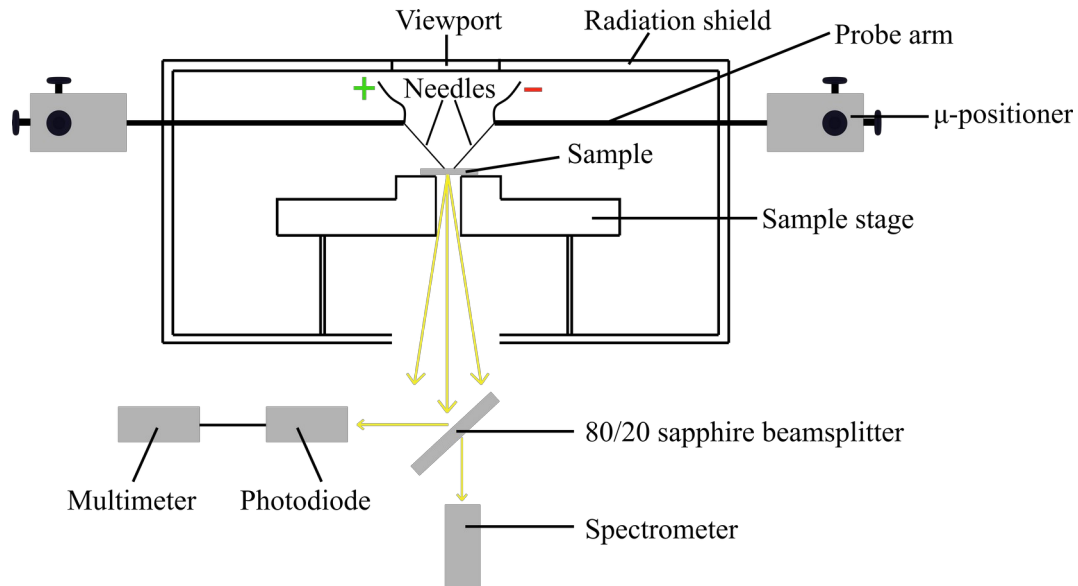
Externe Quanteneffizienz (EQE)



Elektrolumineszenzspektroskopie bei Raumtemperatur

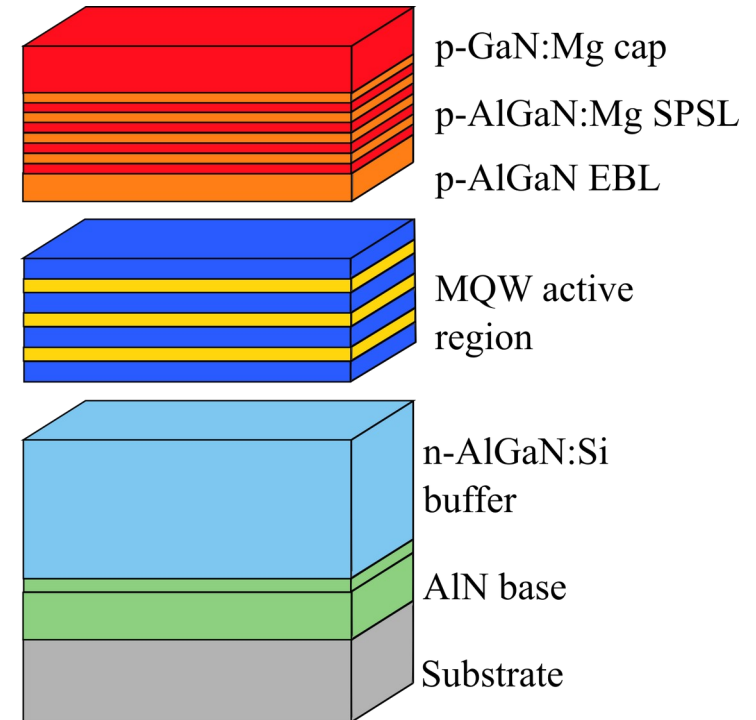


Temperaturabhängige Elektrolumineszenzspektroskopie

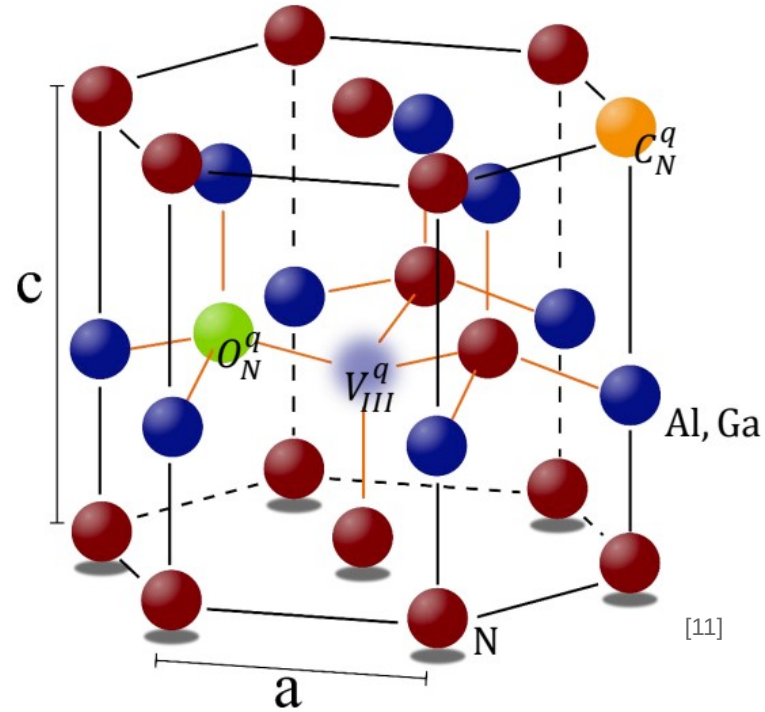


UVC LED Heterostruktur

- Sechs verschiedene Wachstumstemperaturen der aktiven Zone:
900 °C, 935 °C, 970 °C, 1020 °C,
1060 °C, 1100 °C
- Quadratischer p-Kontakt der Größe 0.001 cm²

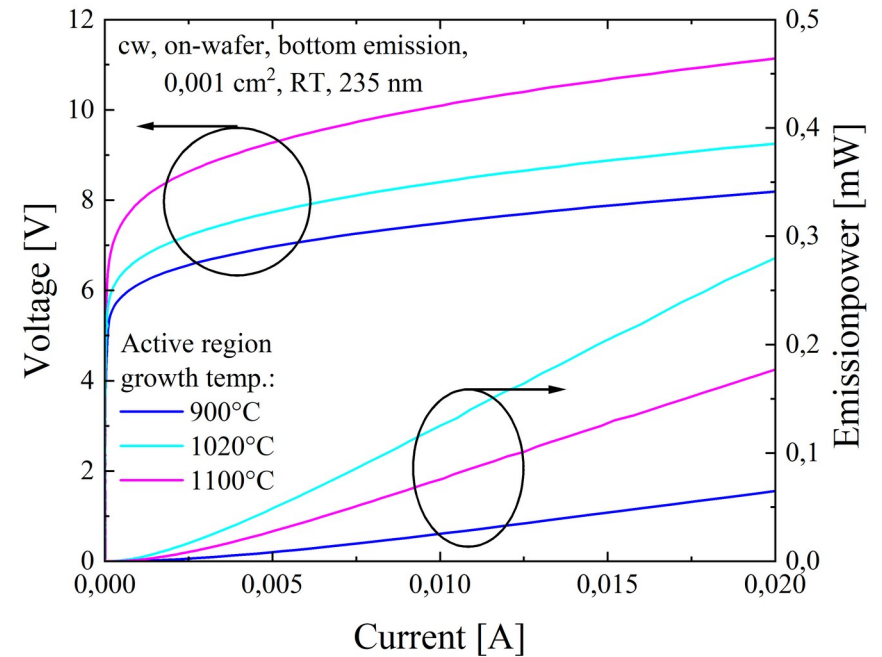
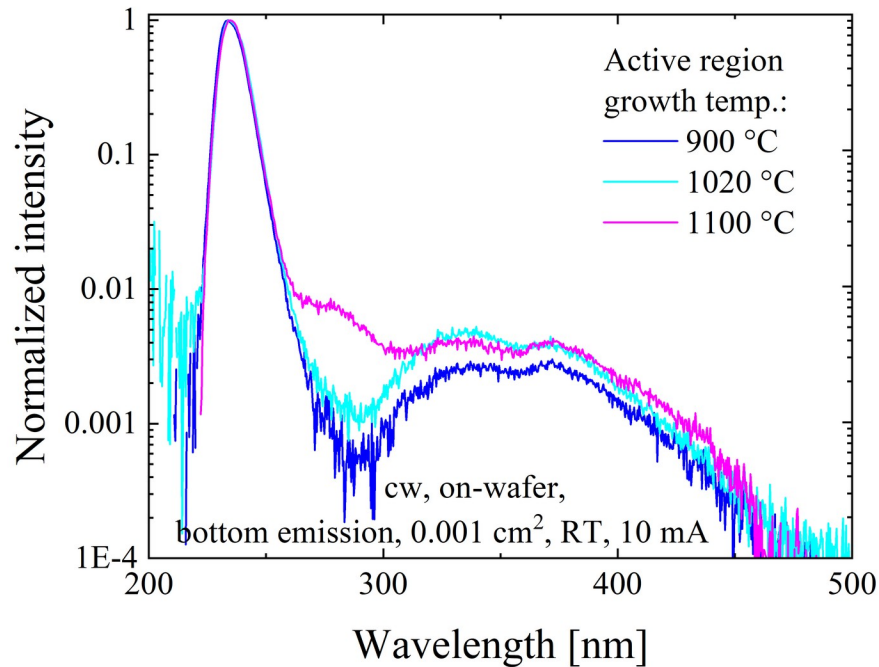


Einbindung von Punktdefekten

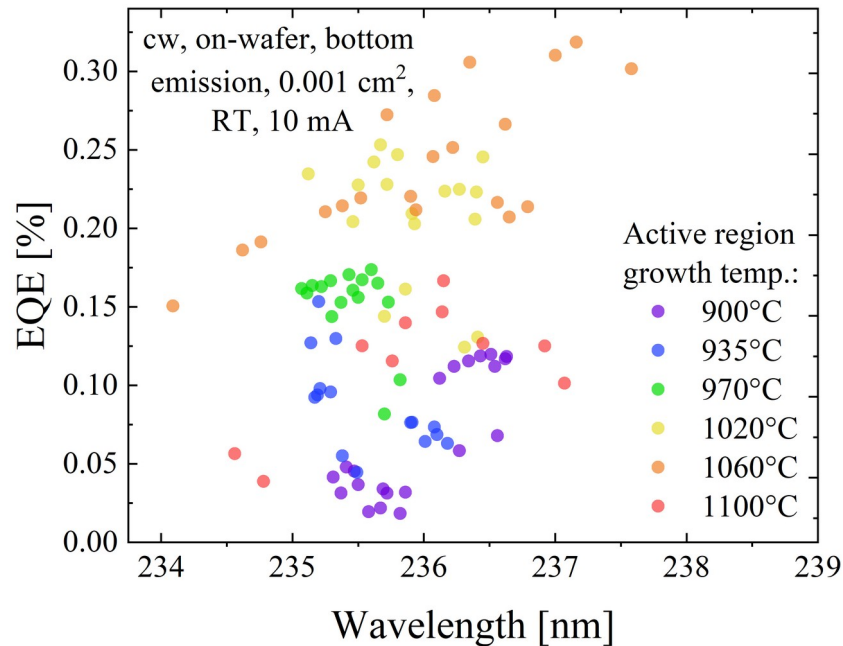


Spektren und LIVs bei Raumtemperatur

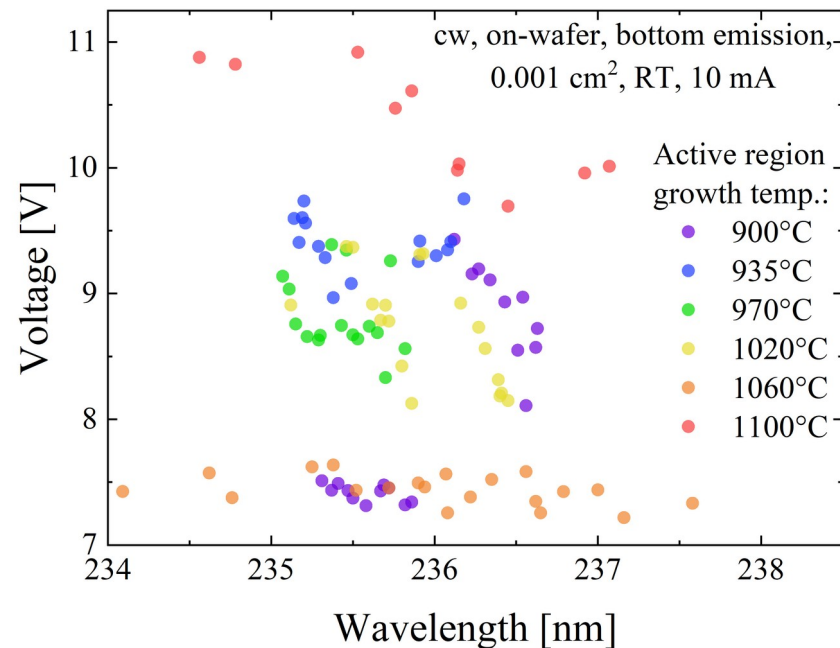
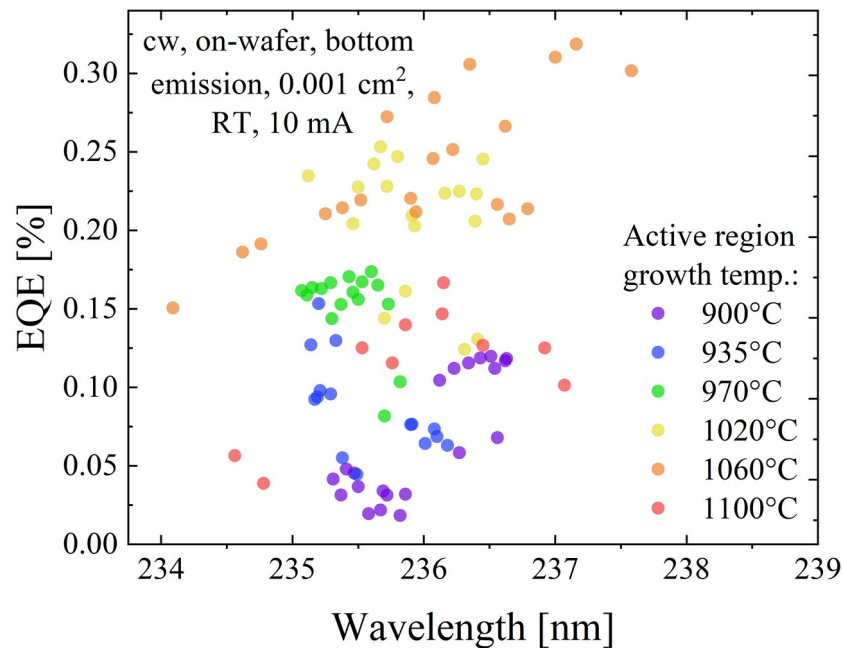
- LIV: light output power (Photostrom)- current (Strom)- Voltage (Spannungs) Kurven



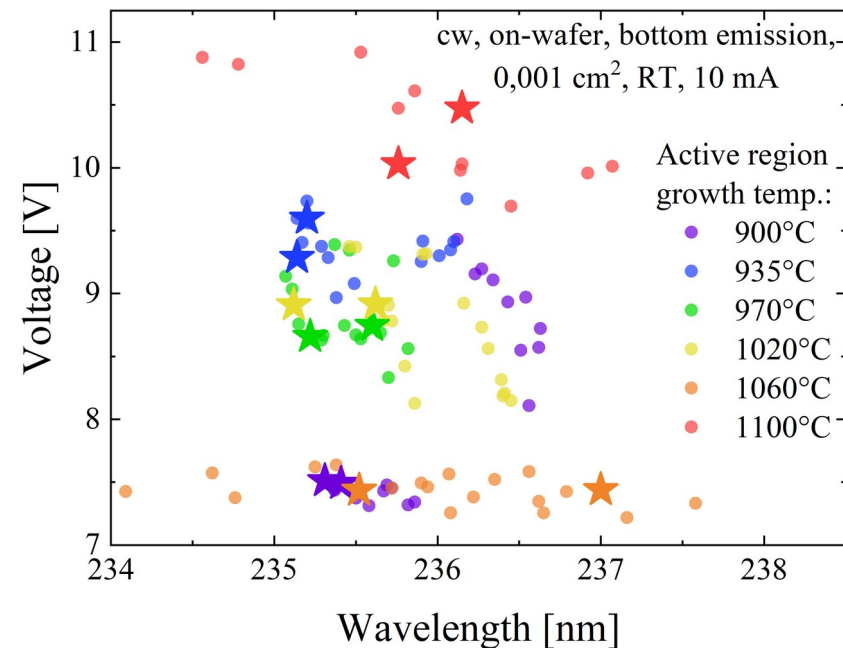
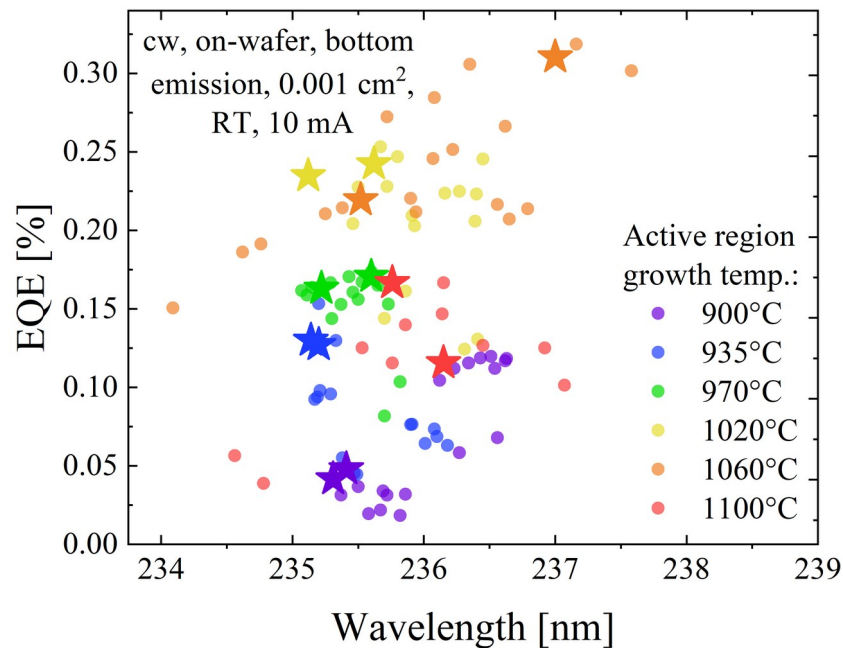
Ergebnisse bei Raumtemperatur



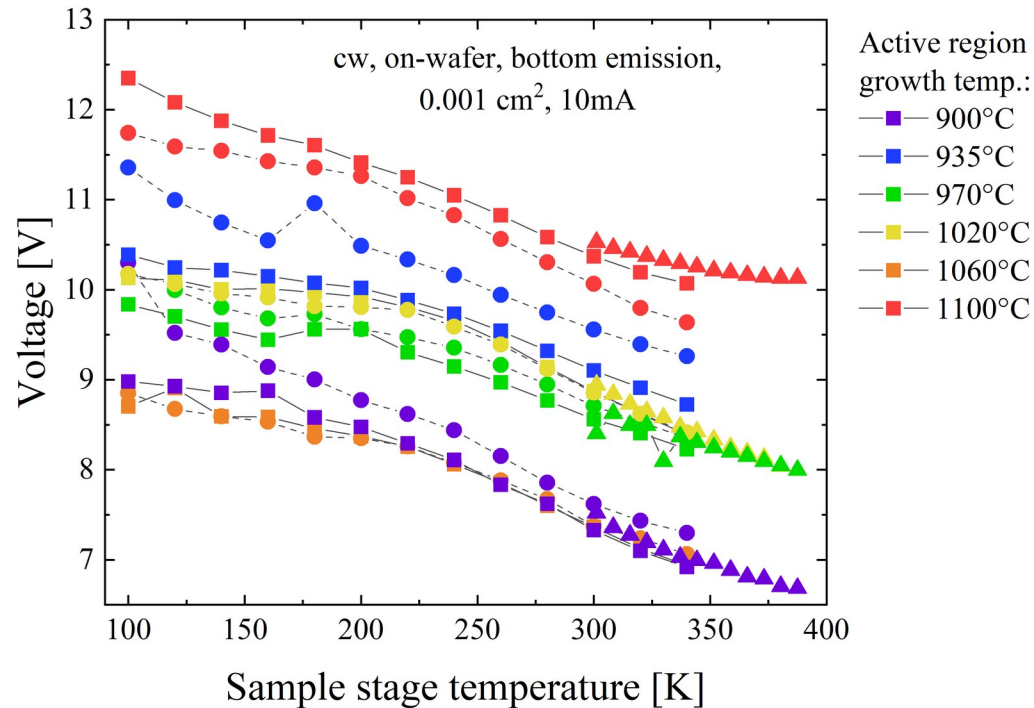
Ergebnisse bei Raumtemperatur



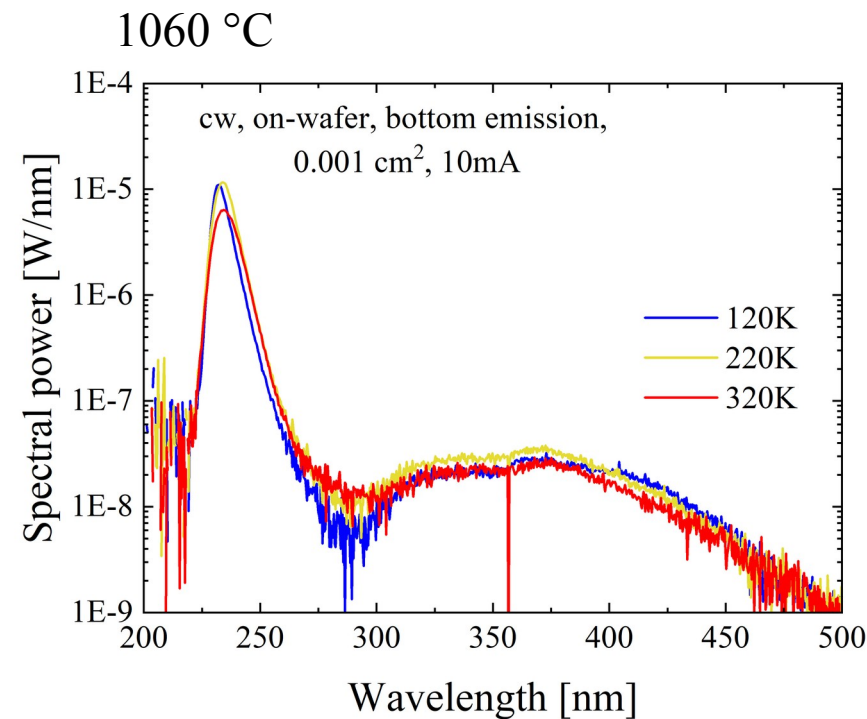
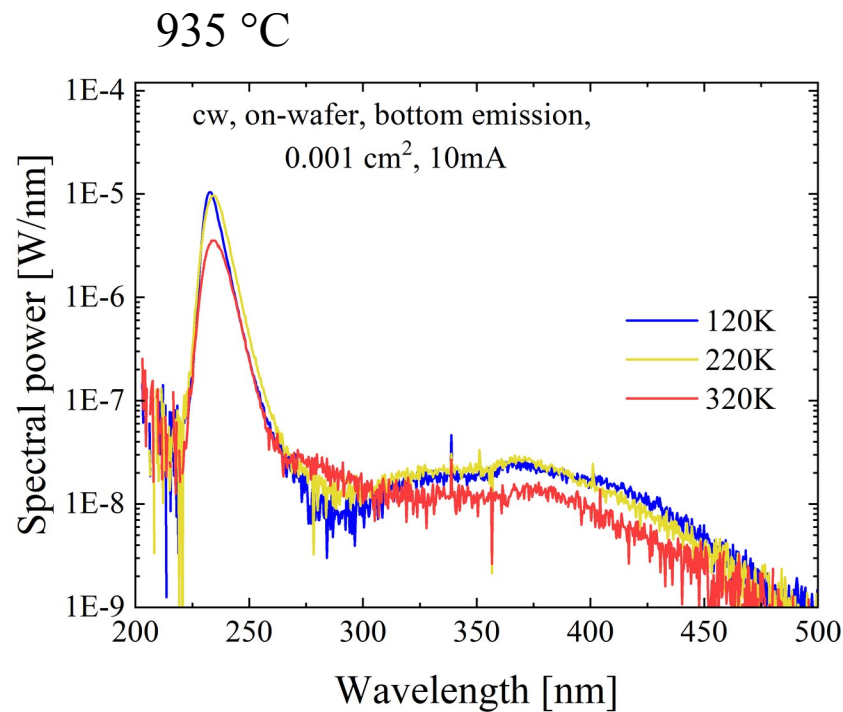
Ergebnisse bei Raumtemperatur



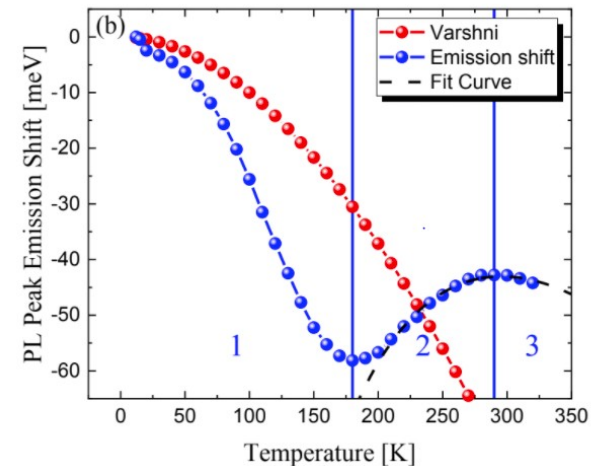
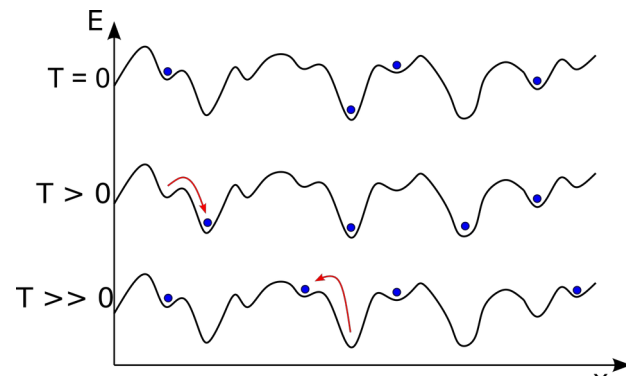
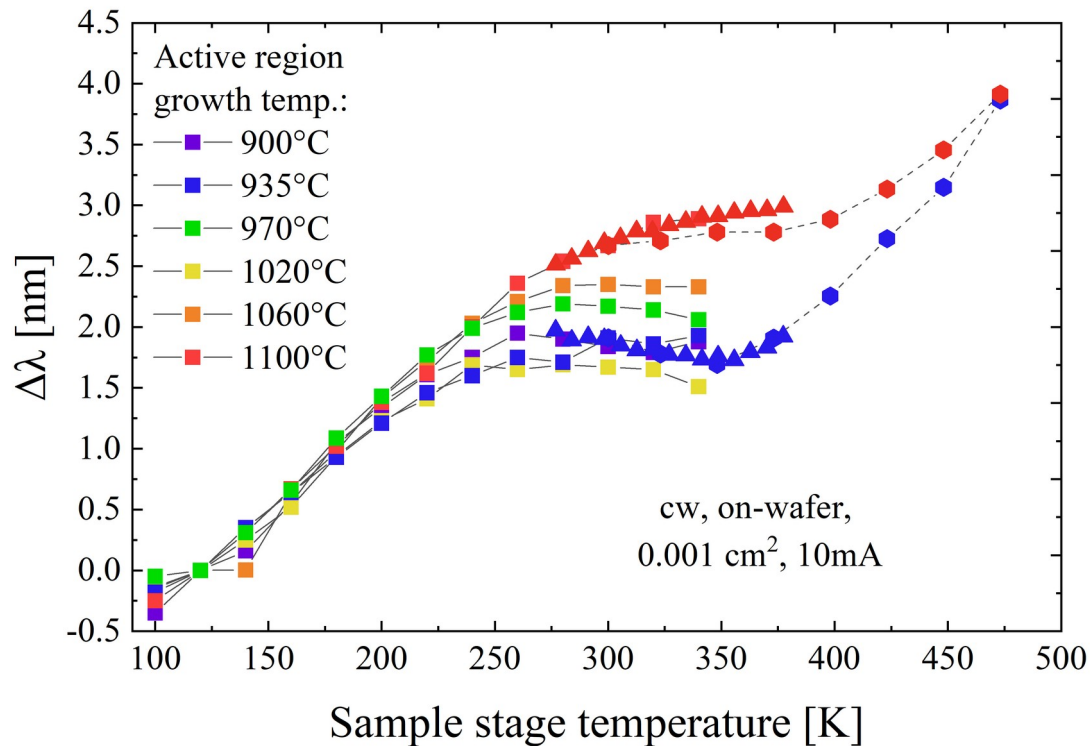
Temperaturabhängige Betriebsspannung bei 10 mA



Temperaturabhängige Spektren

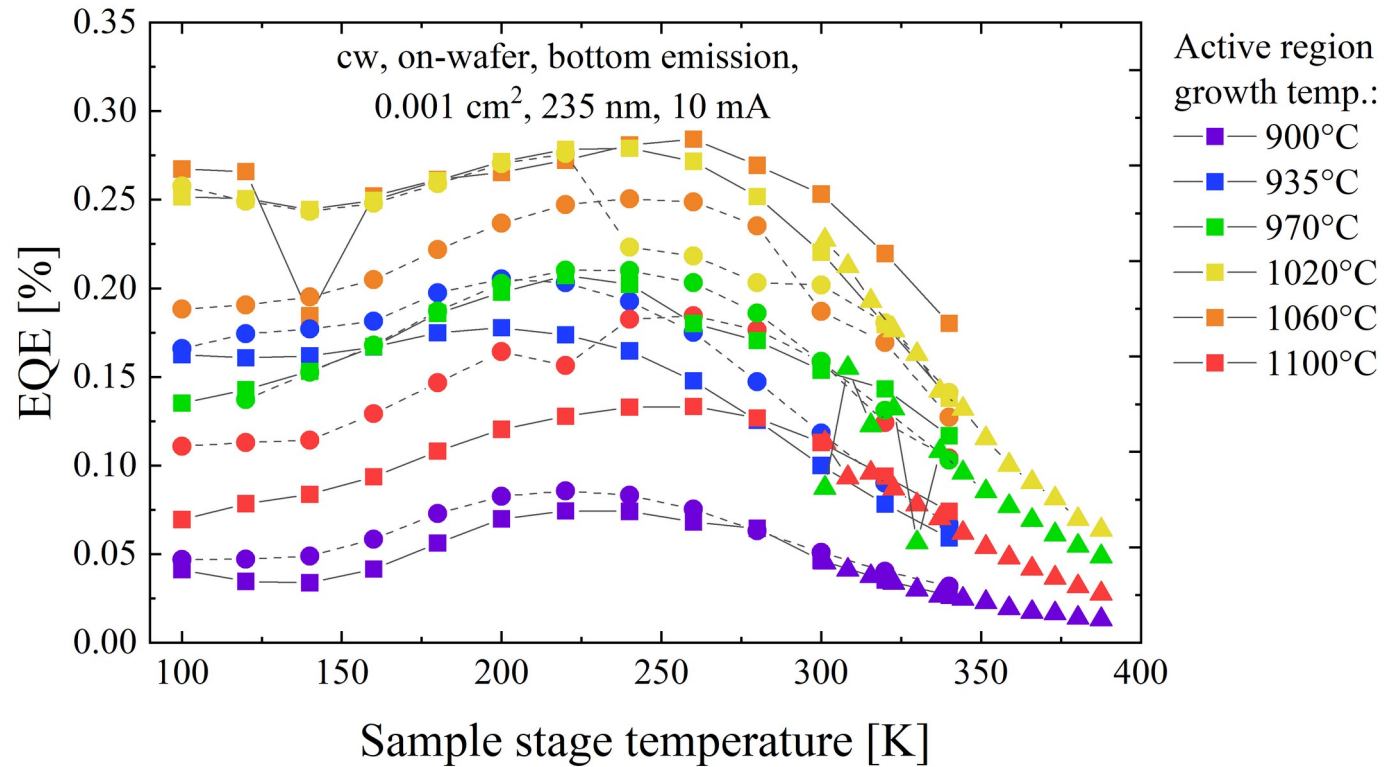


Temperaturabhängige Emissionswellenlänge und Lokalisationseffekte

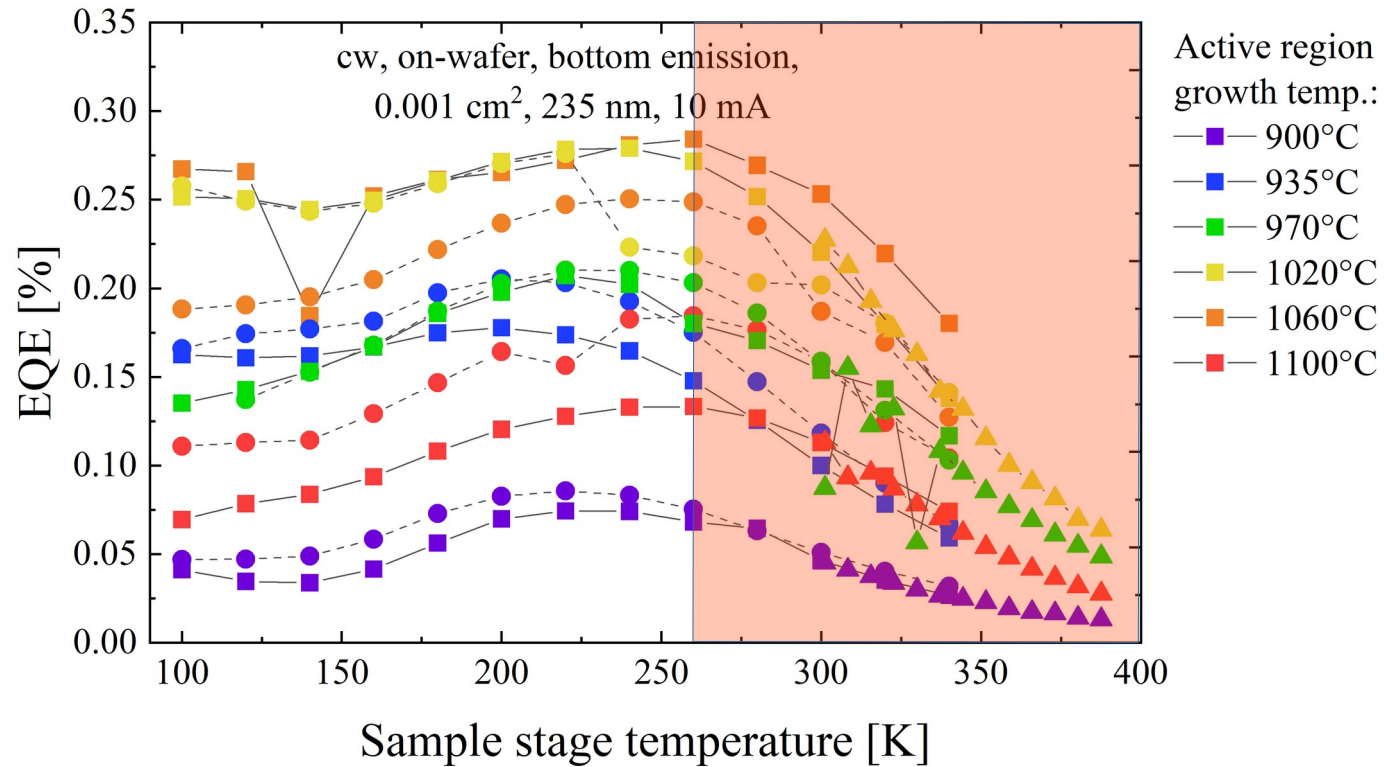


[12]

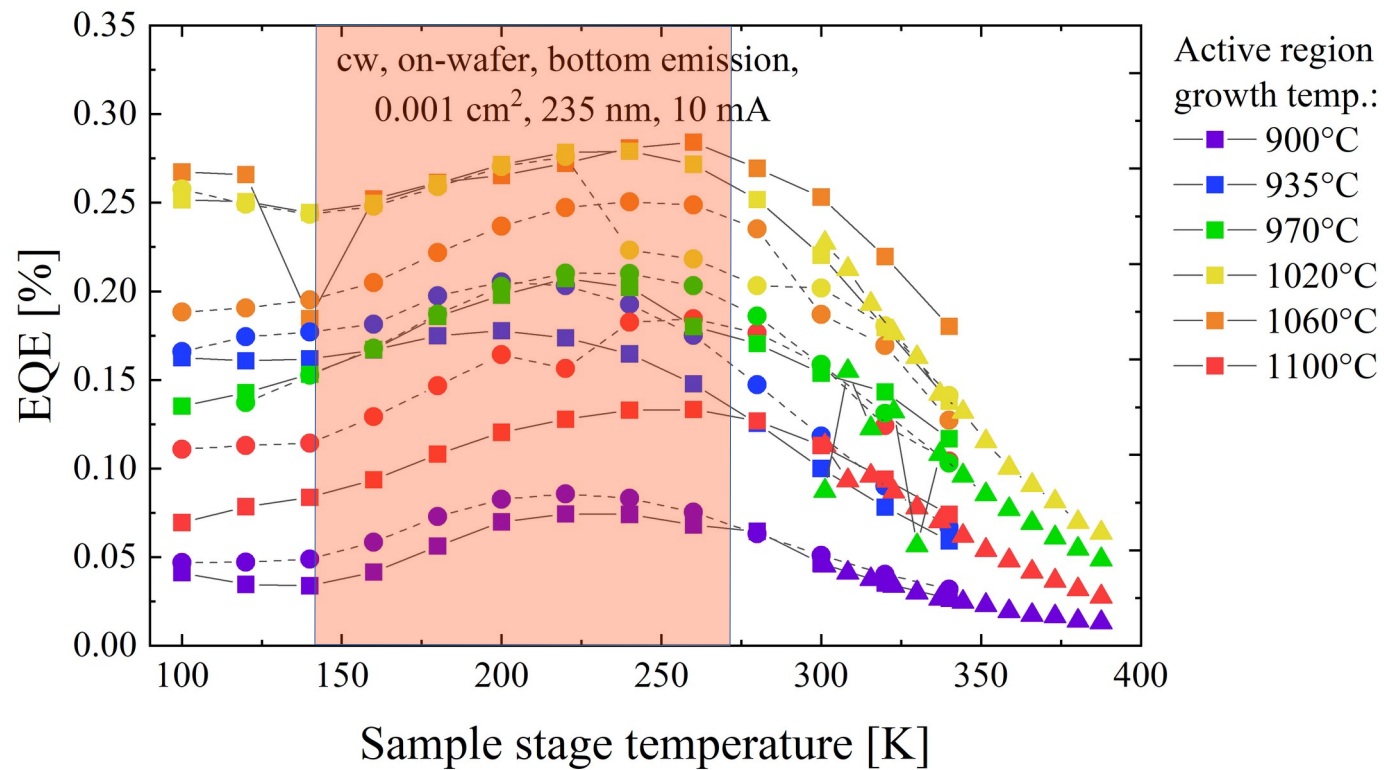
Temperaturabhängige EQE



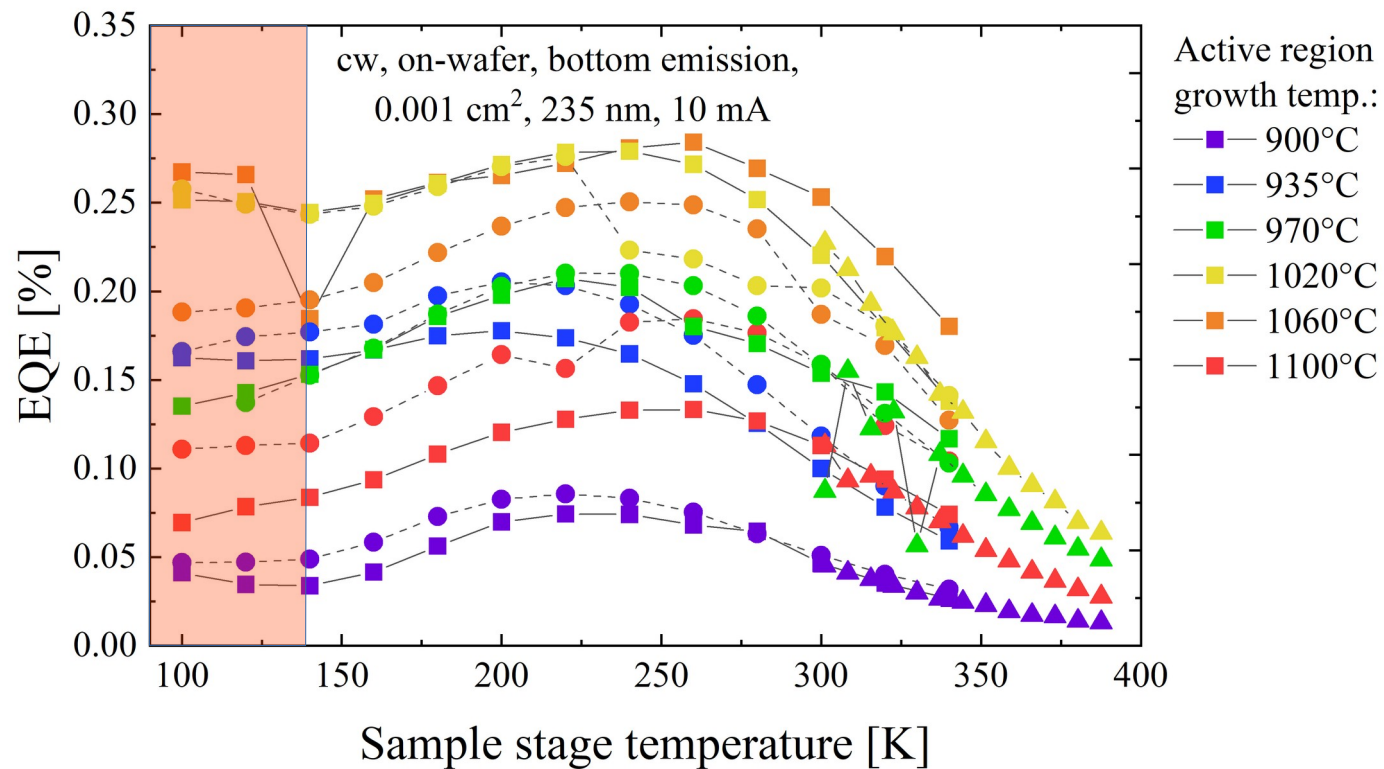
Temperaturabhängige EQE



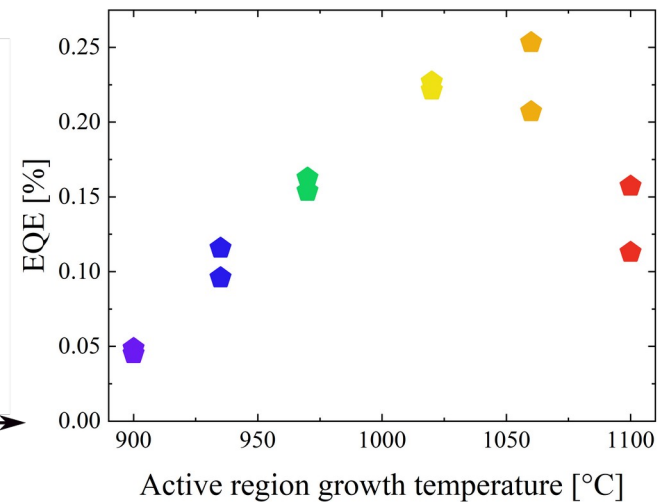
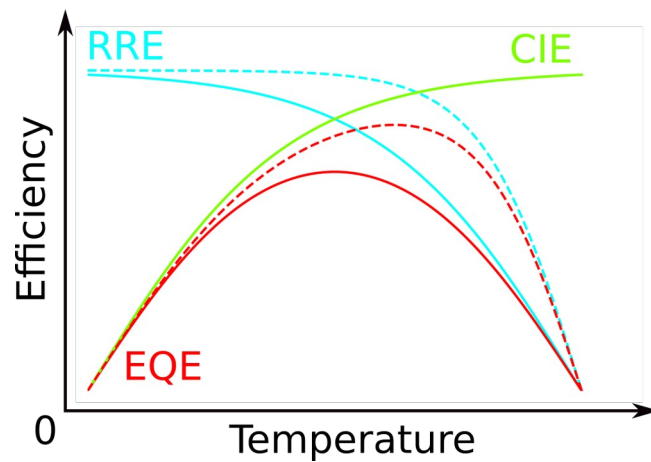
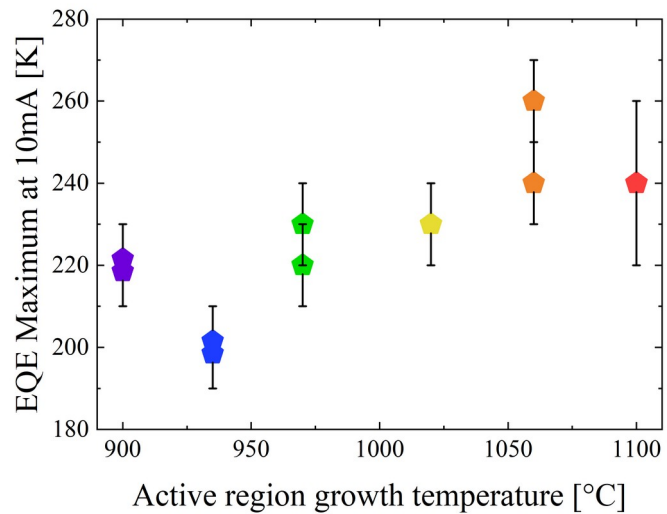
Temperaturabhängige EQE



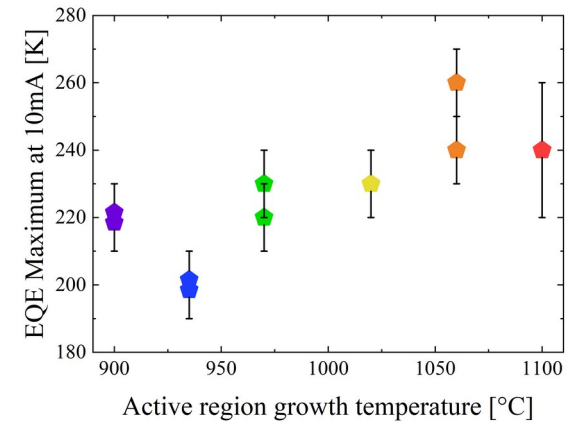
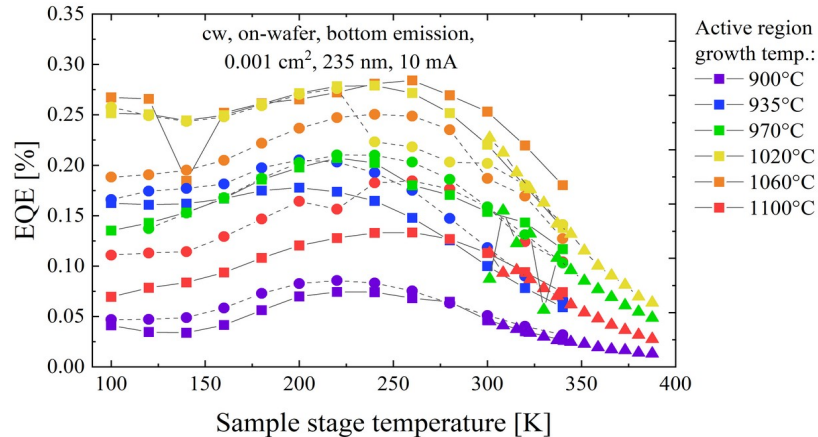
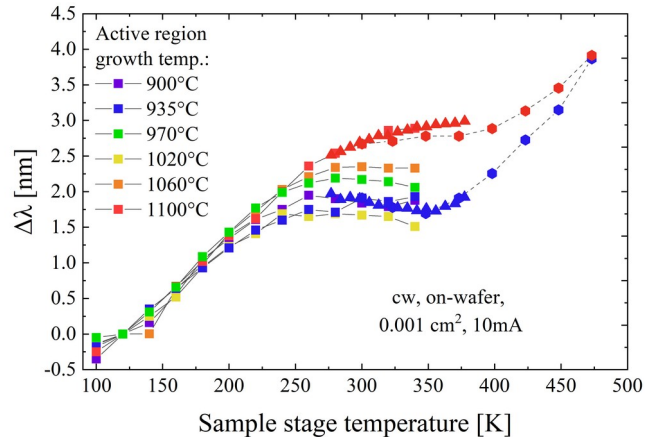
Temperaturabhängige EQE



EQE Maximum



Zusammenfassung und Ausblick



Danke für eure Aufmerksamkeit!

Backup Slides Markus

Quantum well width

- Non-zero polarization, band bending
- Reduction of electron and wavefunctions overlap (QCSE)

- Overlap defines matrix element

$$|M_T|^2 \equiv |\langle u_c | \hat{e} \cdot p | u_v \rangle|^2 |\langle F_2 | F_1 \rangle|^2$$

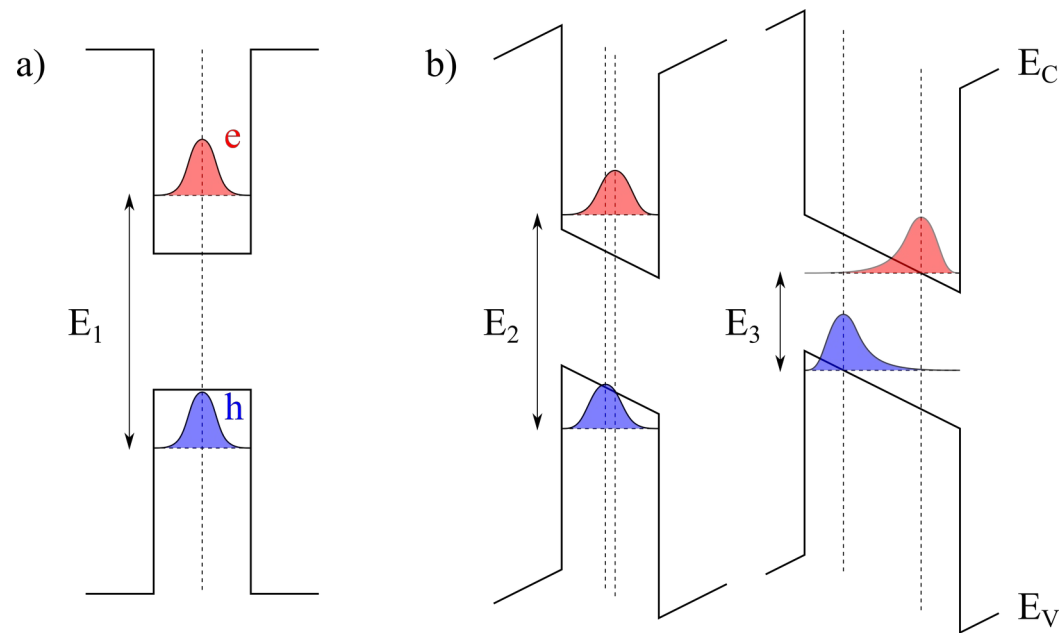
- gain dependent on matrix element

$$g_{21} \propto |M_T|^2 \rho_r(E_{21}) \cdot (f_2 - f_1)$$

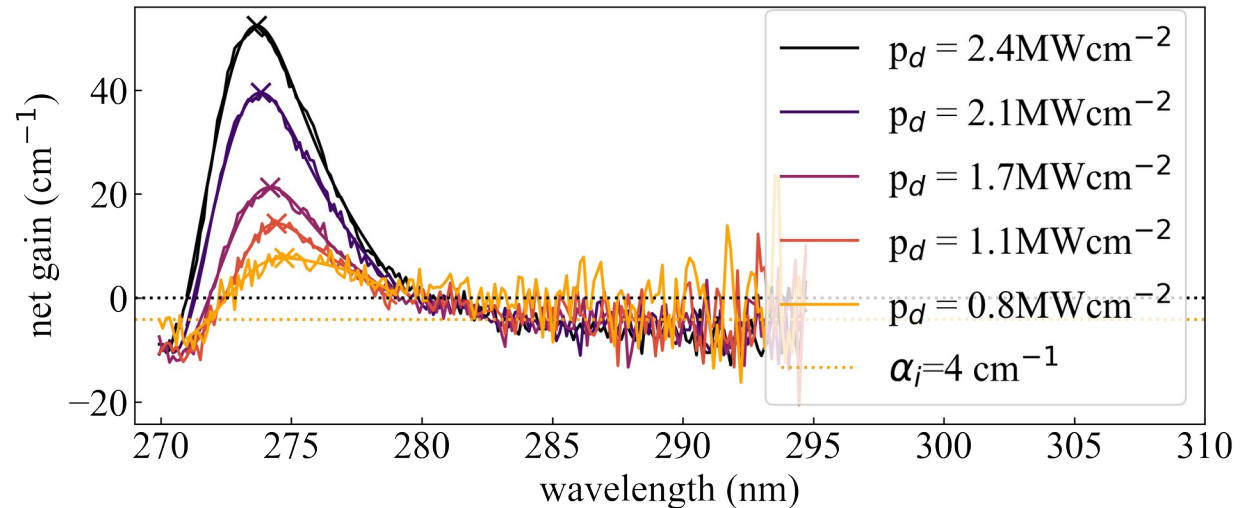
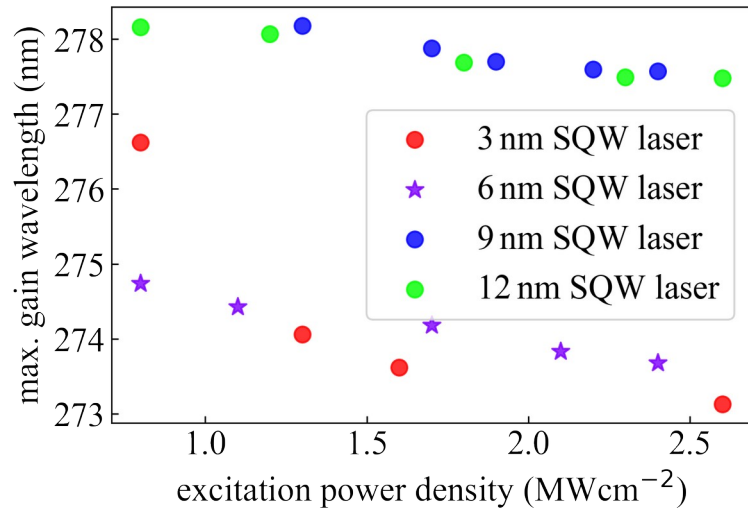
(Fermi's golden rule)

- wider well reduces overlap

→ lower achievable gain



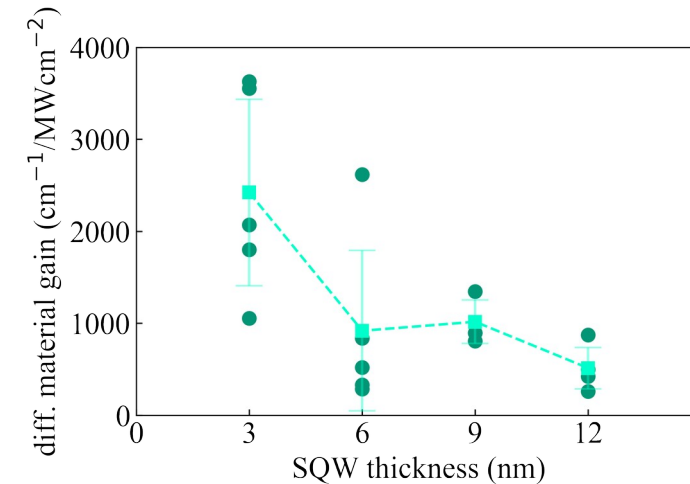
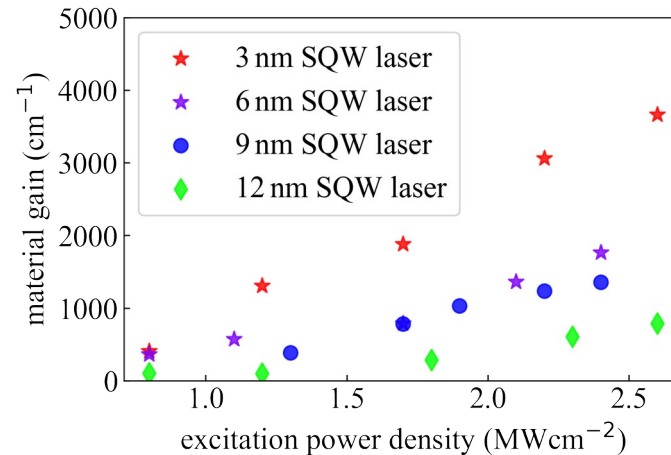
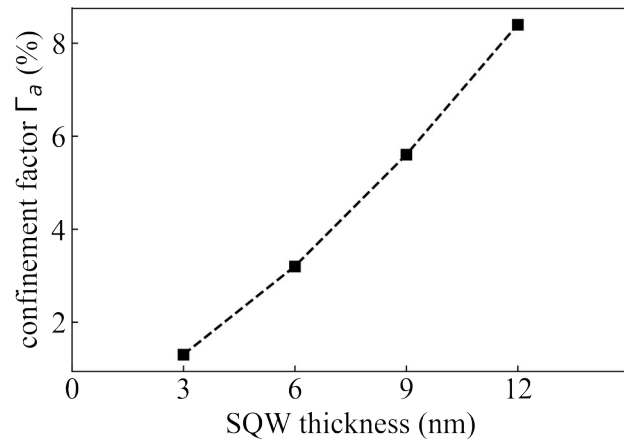
Maximum gain wavelength



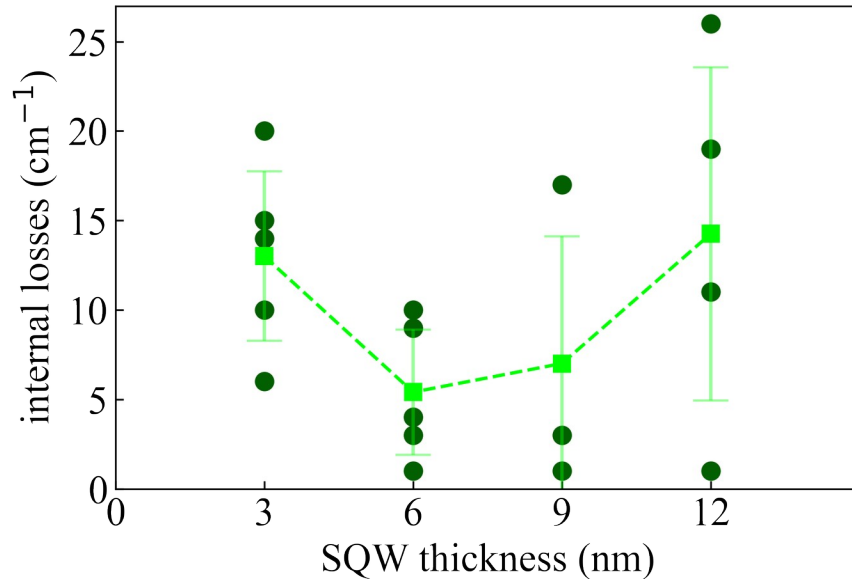
- Blue-shift with increasing excitation power density due to band filling
- Shift more pronounced on lasers with narrower SQWs
- Limited blue-shift rate due to non-resonant pumping → high carrier density in the barriers screening the fields in the in the SQW

Material gain

- Confinement factor defined by overlap between optical mode and active region
- Material gain:
$$g_{mat} = \frac{g_{mod}}{\Gamma_a} = \frac{g_{net} + \alpha_i}{\Gamma_a}$$
- material gain and differential material gain mirror confinement factor

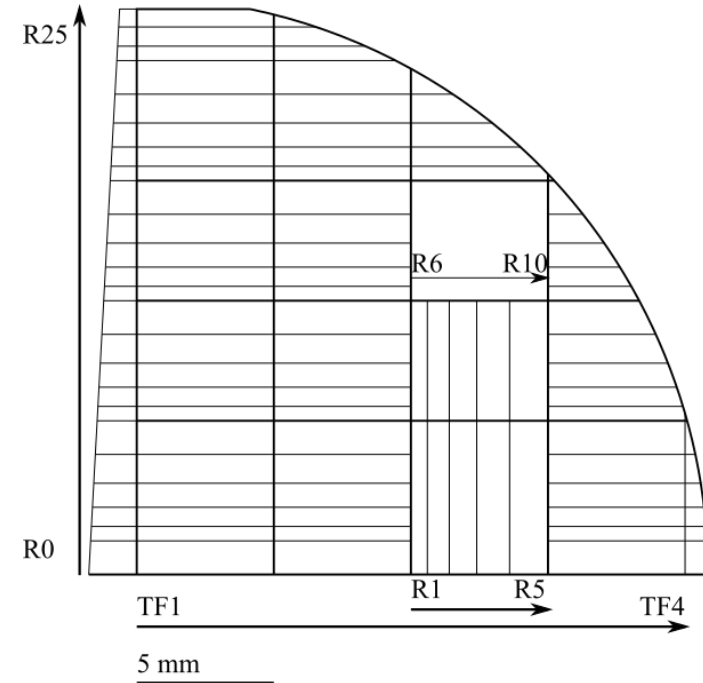
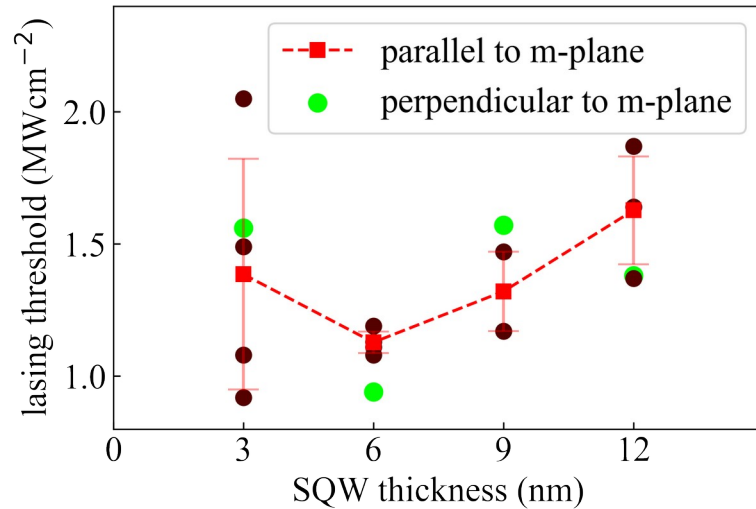


Internal losses



- Internal losses comparable on different lasers
- Trend follows the threshold power density
- Scattering in losses attributed to lateral variation of epitaxial structure

Influence of facet orientation



- Laser bars with different orientations
- Dependent on m-plane, a-plane and ELO stripes
- no apparent change in threshold

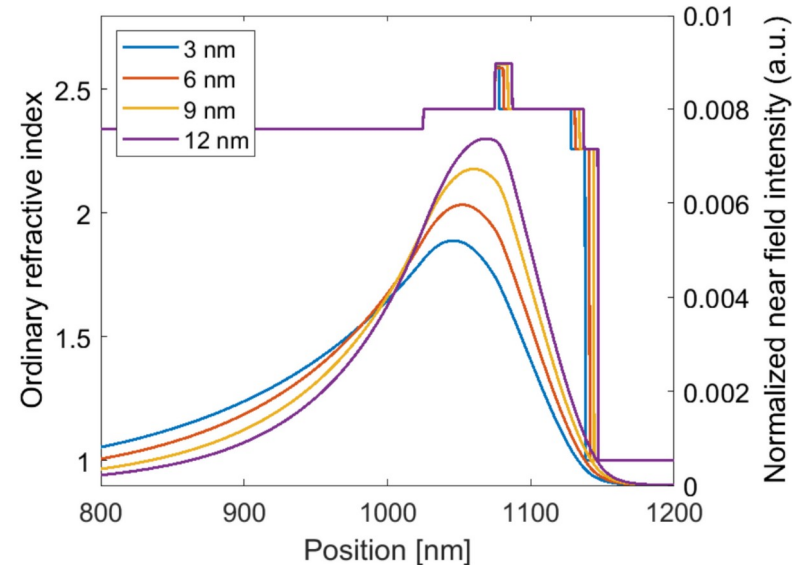
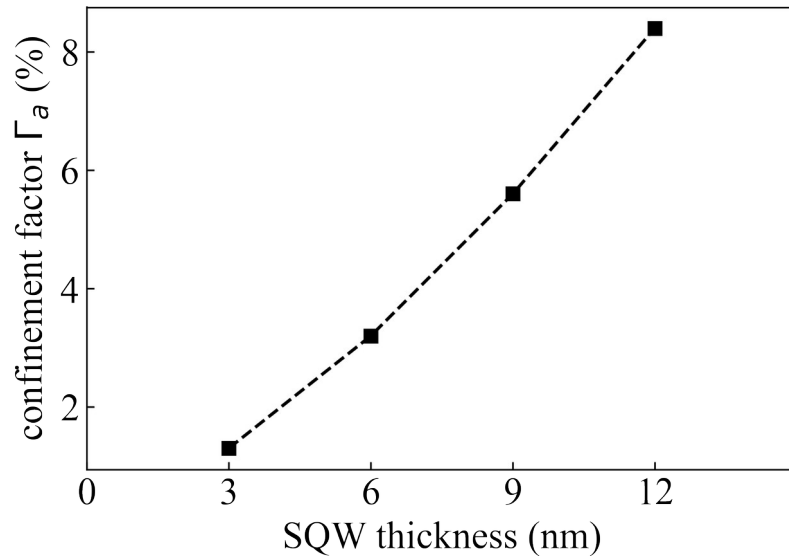
Edge-Emitting Lasers (EELs)

- Laser cleaved facets acting as semi-transparent resonator mirrors
- Constructive interference on light (cavity modes)
- Emission wavelength defined by the mode, for which gain is higher than losses
- Emission through the edge
- Cavity length of EELs can be easily varied
- Elliptical output beam

AlN 10 nm cap
Al _{0.63} Ga _{0.37} N 50 nm p-WG
Al _x Ga _{1-x} N y nm SQW
Al _{0.63} Ga _{0.37} N:Si 50 nm n-WG
Al _{0.76} Ga _{0.24} N:Si 900 nm cladding
Al _{0.76} Ga _{0.24} N 100 nm buffer
AlN-Al _{0.76} Ga _{0.24} N 25 nm buffer
HTA/ELO AlN/sapphire substr.

Optical Gain

- Material gain defined by Fermi's golden rule $g_{mat} \propto |M_T|^2 \rho_r(E_{21}) \cdot (f_2 - f_1)$
- Modal gain: $g_{mod} = \Gamma \cdot g_{mat}$ with confinement factor Γ
- Net gain is measured and includes losses: $g_{net} = g_{mod} + \alpha_i$

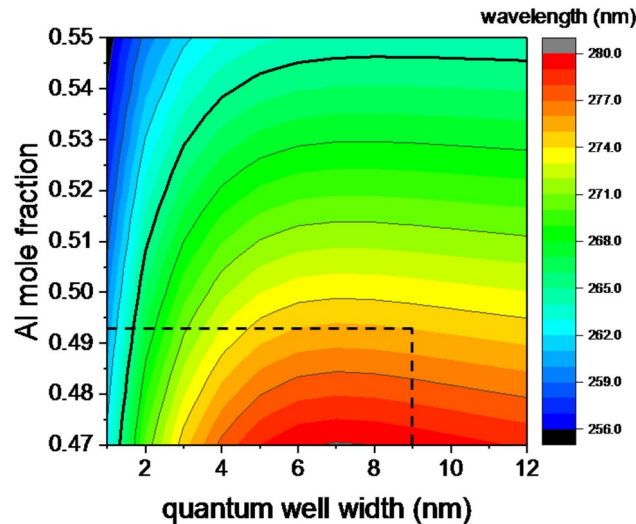


Laser structure

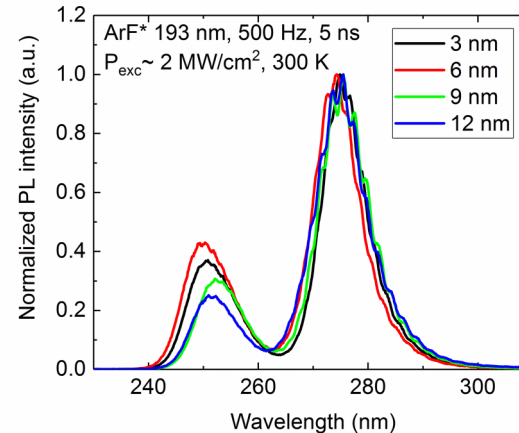
AlN 10 nm cap
Al _{0.63} Ga _{0.37} N 50 nm p-WG
Al _x Ga _{1-x} N y nm SQW
Al _{0.63} Ga _{0.37} N:Si 50 nm n-WG
Al _{0.76} Ga _{0.24} N:Si 900 nm cladding
Al _{0.76} Ga _{0.24} N 100 nm buffer
AlN-Al _{0.76} Ga _{0.24} N 25 nm buffer
HTA/ELO AlN/sapphire substr.

TS number	x	y
5873	0.438	3
5858	0.446	6
5877	0.433	9
5862	0.429	12

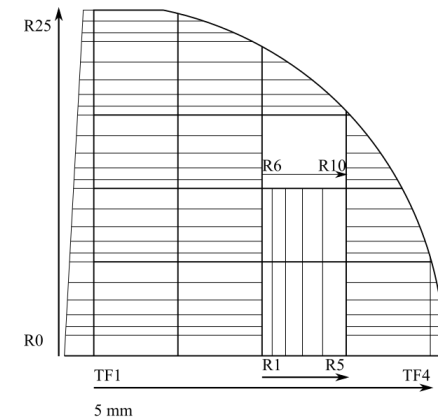
- AlGa_N-based optically-pumped lasers with SQW active region (3 nm, 6 nm, 9 nm, 12 nm)
- Al molar fraction in SQW calibrated to emit at 275 nm at 2 MW/cm²
- Laser scribing into single laser bars



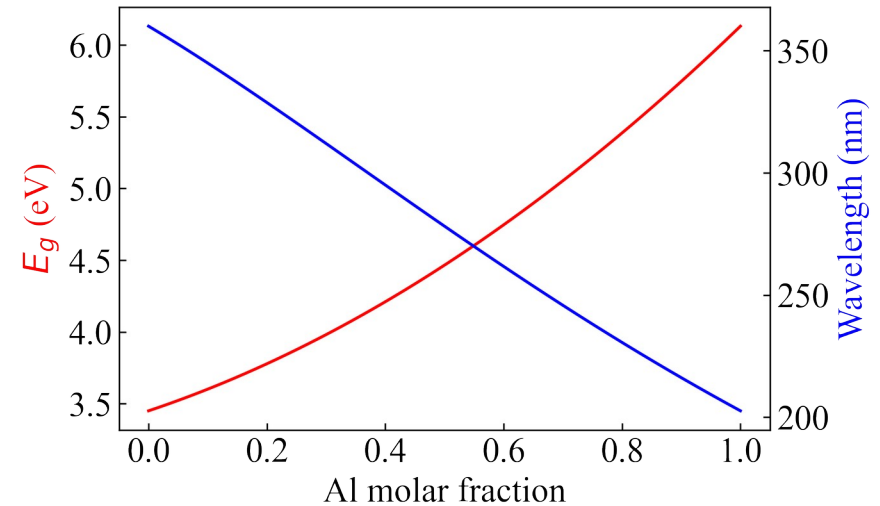
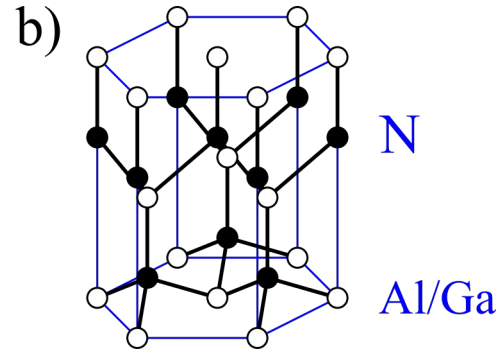
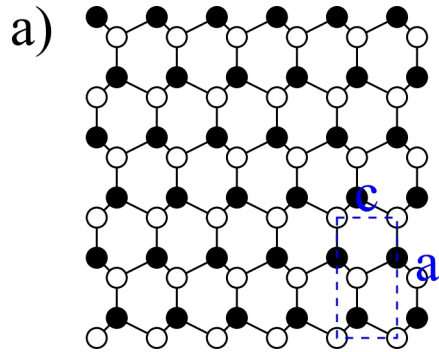
Simulation by M. Guttman



Measurements by G. Cardinali



AlGaN material system

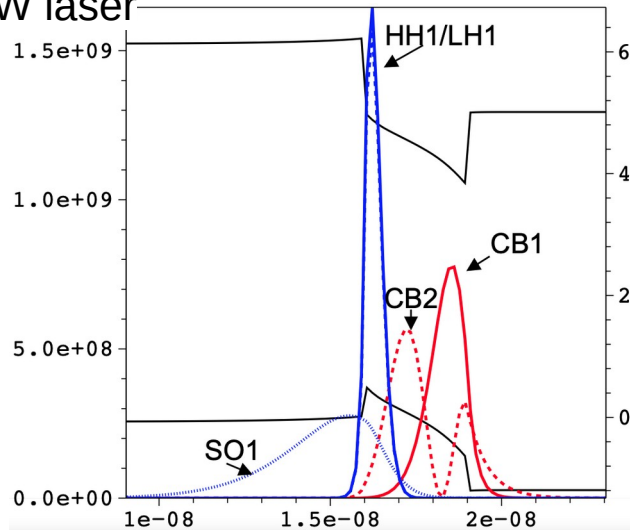


- Wurtzite crystal structure
- AlGaN energy bandgap dependent on Al molar fraction, is calculated by Vegard's law
- Non-zero net dipole moment (spontaneous polarization)
- Growth of strained layers with different lattice constants causes piezoelectric polarization

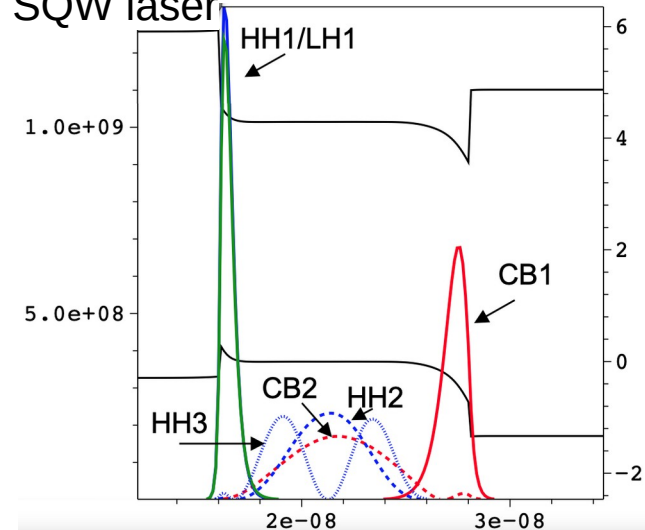
$k \cdot p$ simulations

- Simulations by B. Witzigmann
- Polarization fields screening by fundamental states for thicker QWs

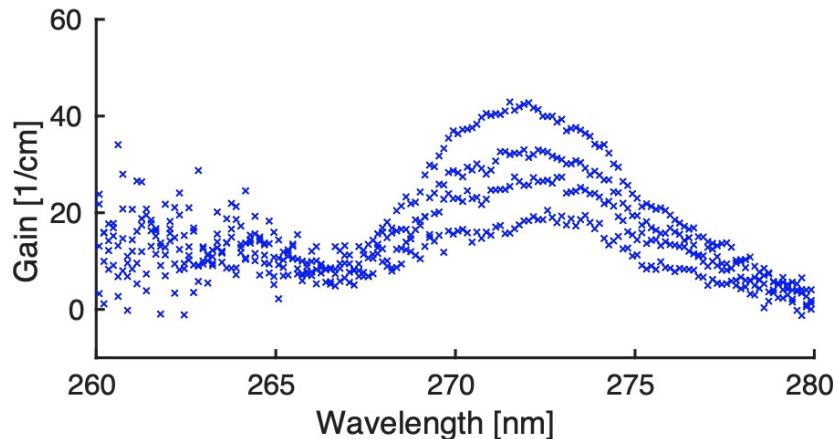
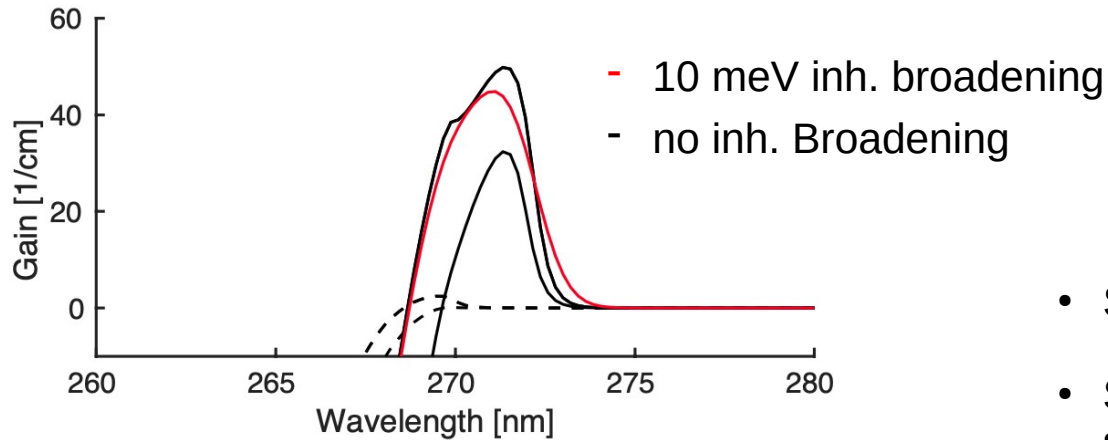
3 nm SQW laser



12 nm SQW laser

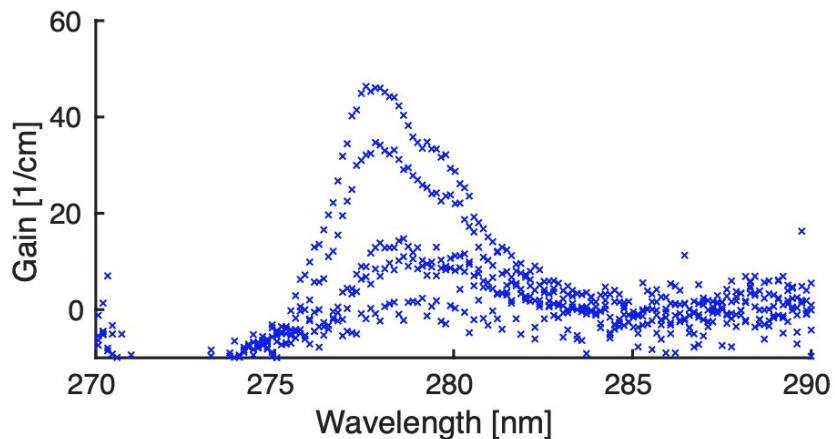
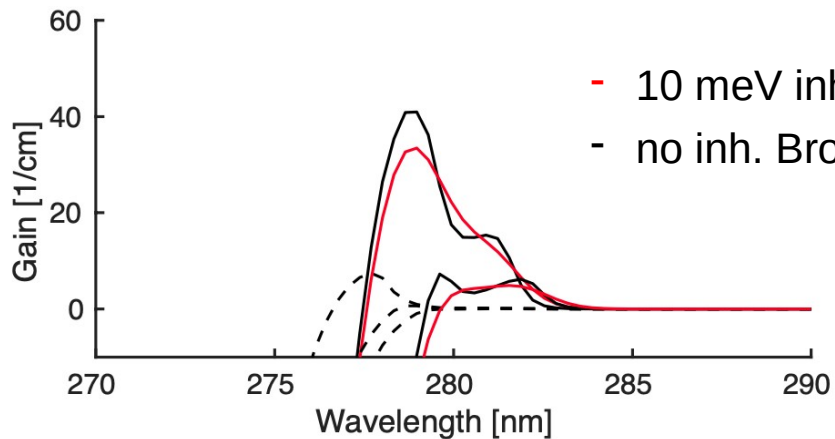


Gain Simulation 3nm



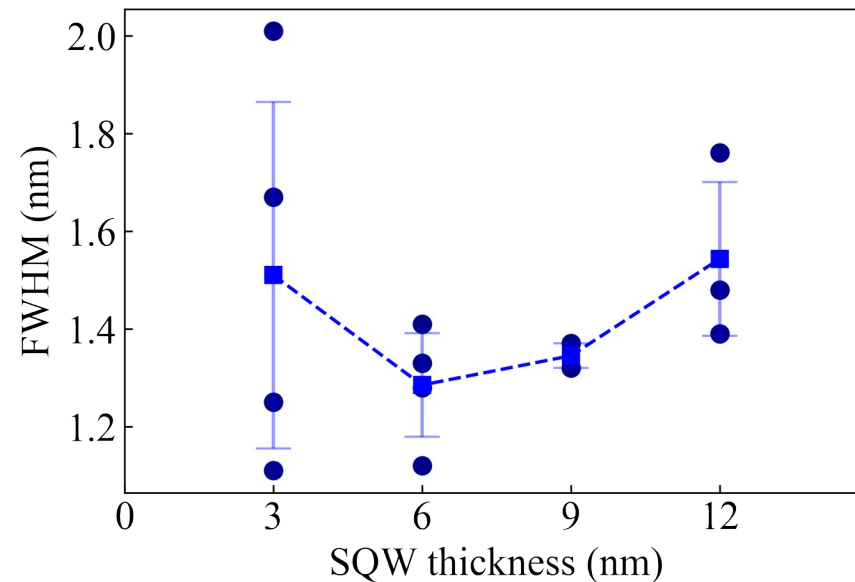
- Simulation by B. Witzigmann
- Screened Hartree-Fock approximation (5 meV state broadening)
- Reduced polarization charges
- Main transitions:
 - $\langle e1|h1 \rangle$ and $\langle e1|h2 \rangle$

Gain Simulation 12nm



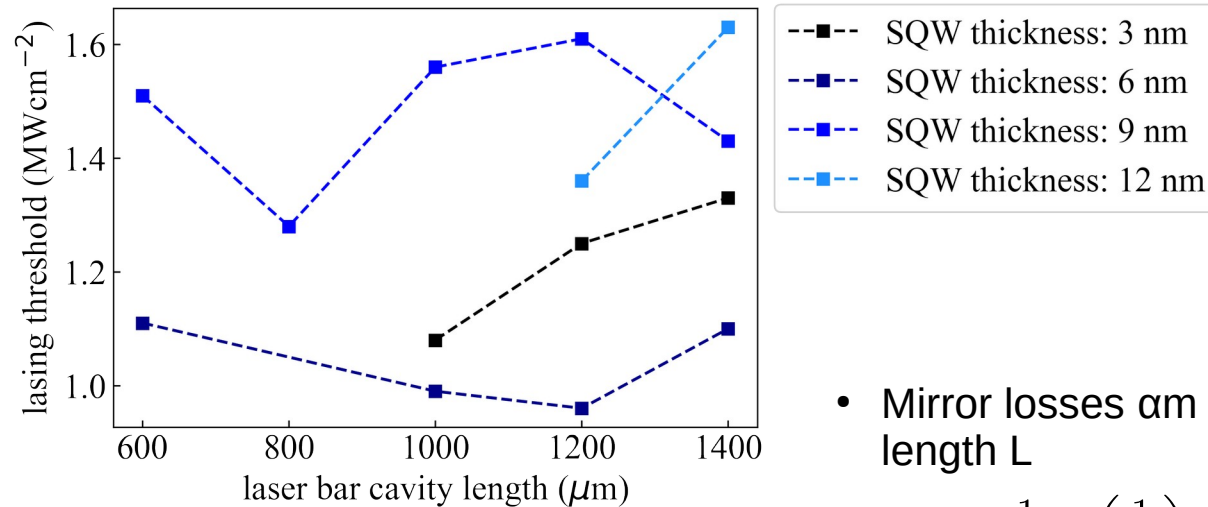
- Simulation by B. Witzigmann
- Screened Hartee-Fock approximation (5 meV state broadening)
- Reduced polarization charges
- Main transitions:
 - $\langle e1|h2 \rangle$ and $\langle e2|h3 \rangle$

Full width at half maximum (FWHM)



- Determined by gaussian fit of emission peaks
- FWHM below 2 nm for all samples

Influence of cavity length



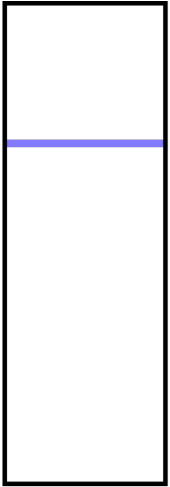
- Mirror losses α_m increase with decreasing cavity length L

$$\alpha_m = \frac{1}{L} \ln \left(\frac{1}{R} \right)$$

- Higher losses for gain to overcome should increase threshold with decreasing cavity length
- Trend not noticeable

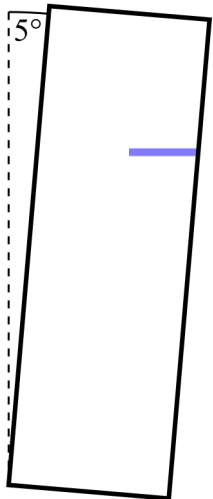
Measurements

a)



- Power series
- Lasing threshold measurements:
 - Spectra for various excitation power densities
 - Full cavity pumped, stripe perpendicular to edge (a)

b)

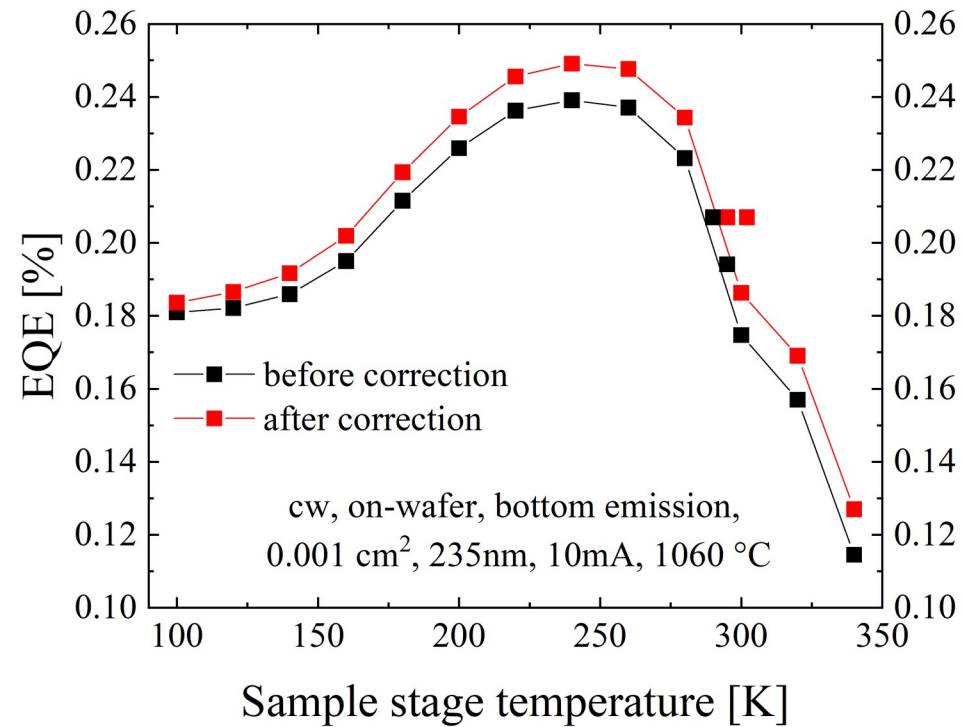
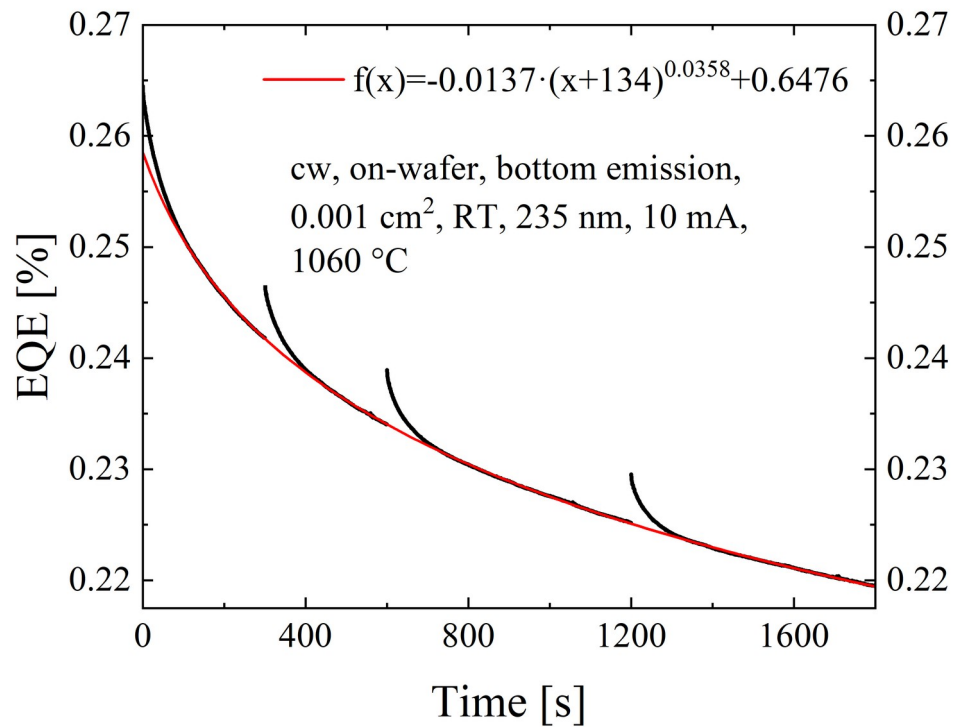


- Variable stripe length method:
 - Spectra taken for several stripe lengths (50 μm - 500 μm)
 - Repeated for few excitation power densities
 - Sample at an angle to avoid resonance (b)

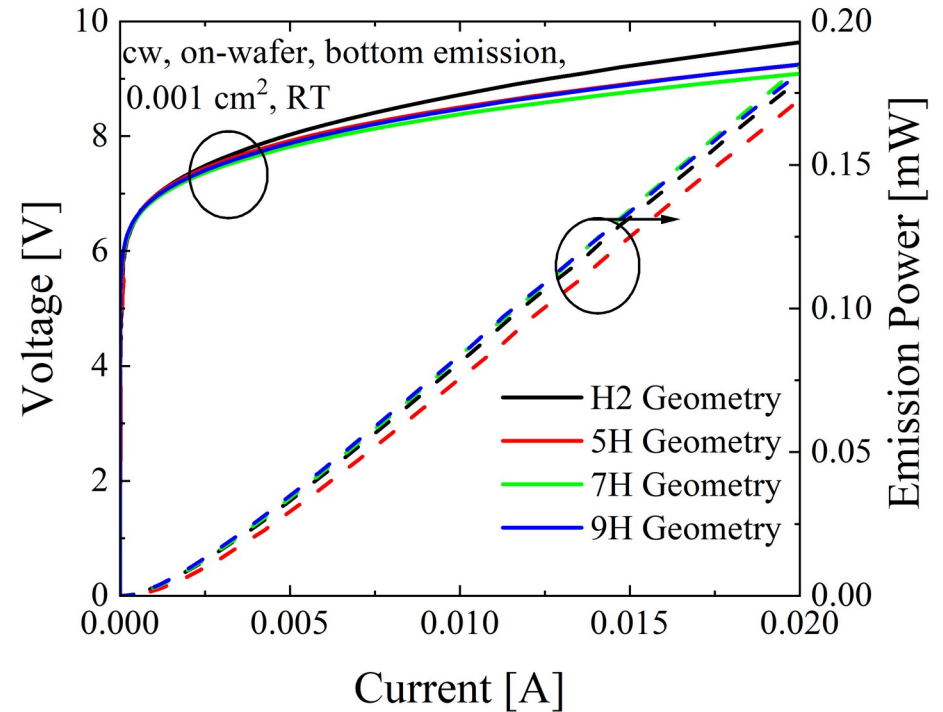
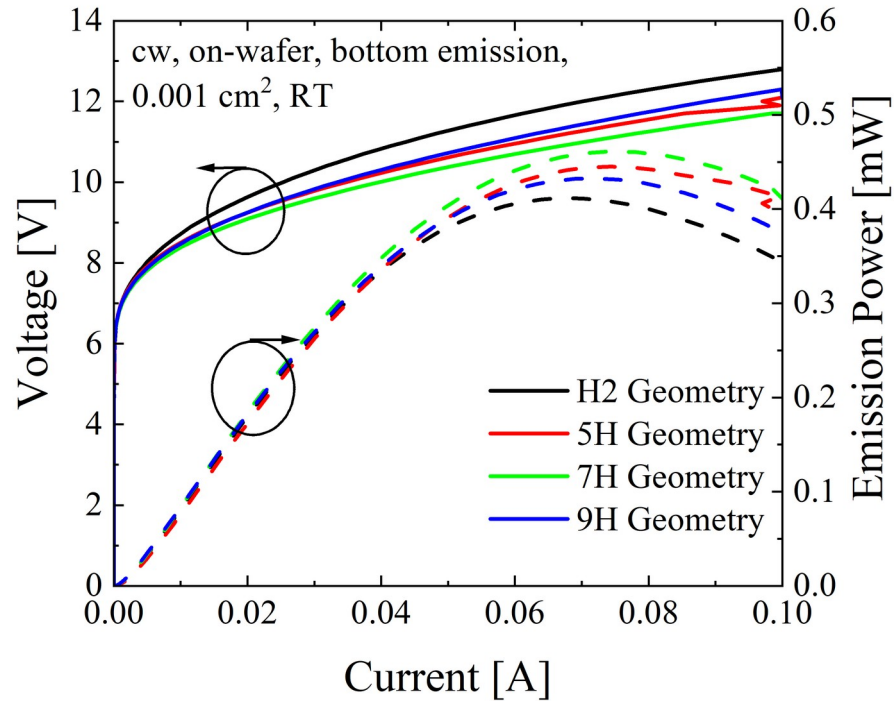
Backup Slides Paula



Alterungseffekte



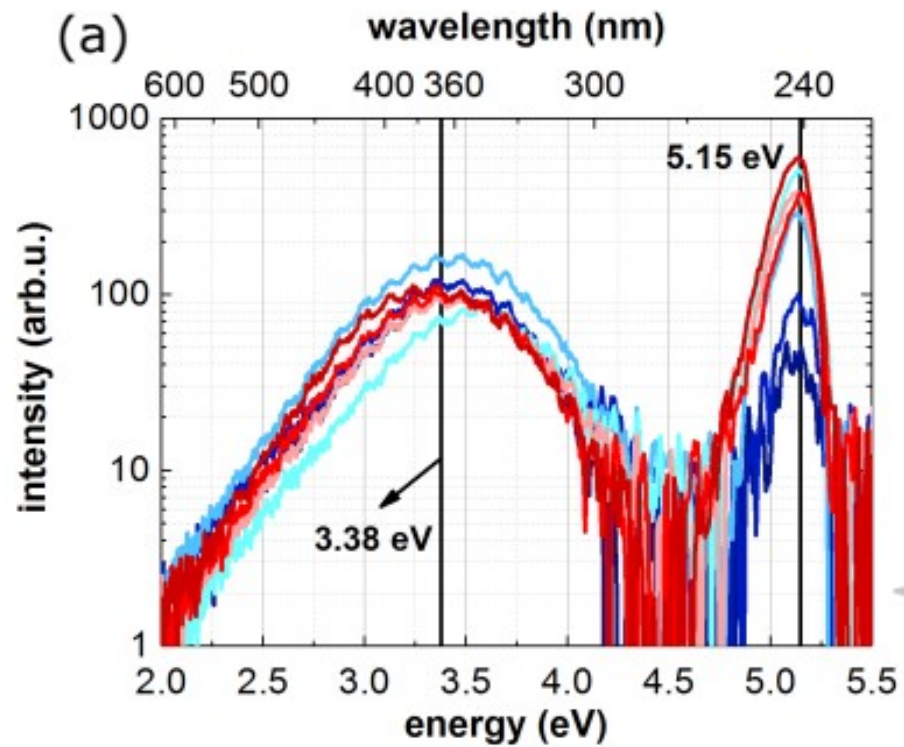
Kontaktgeometrie



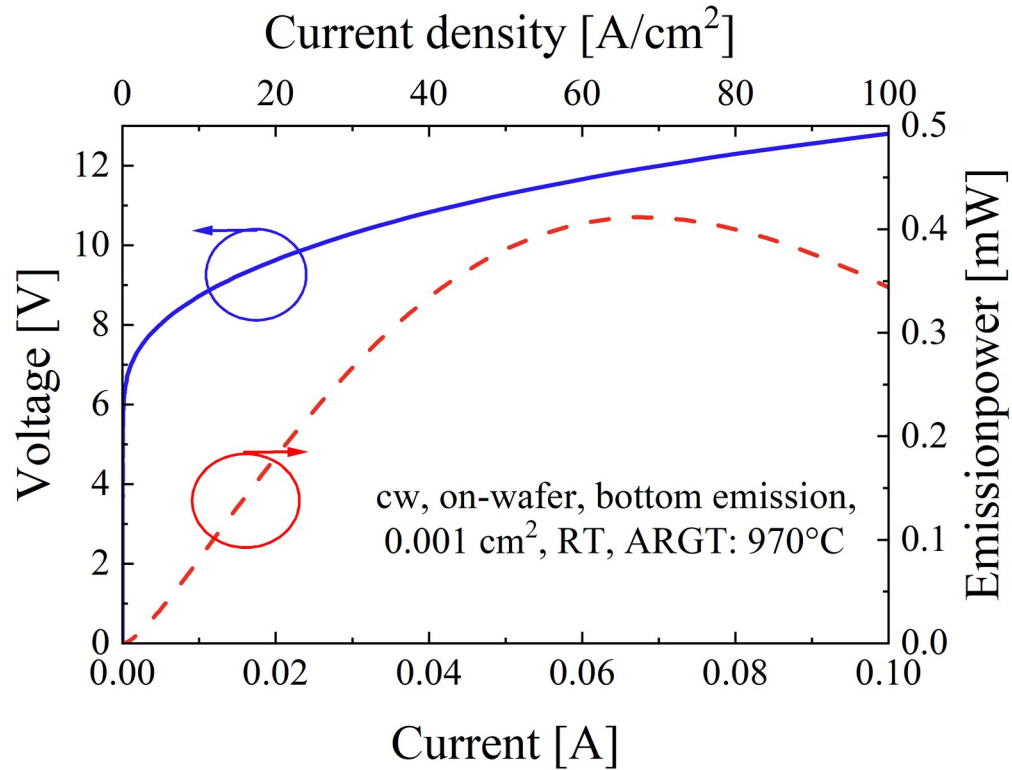
Struktur

Layer	x [%]	d [nm]	Doping	Remarks
GaN:Mg	0	300	2%	Cap
14x (Al _x Ga _{1-x} N:Mg / Al _y Ga _{1-y} N:Mg)	80/70	25 (0.9/0.9)	5E-3/4.4E-3	p-SPSL
AlGaN	100	6	-	EBL
AlGaN	83.5	5	-	last barrier
2 x AlGaN(:Si)	83.5	5	2.02E-4	barriers
3 x AlGaN	70	1	-	QW
AlGaN:Si	83.5	40	4.02E-4	first barrier
AlGaN:Si	87	2200	1E-4	n-side buffer
AlGaN	87	100	-	Buffer
AlN-AlGaN transition	100→87	25	-	Buffer transition
AlN	100	400	-	Smooth buffer
HTA ELO-tmpl.			-	

PL Measurements

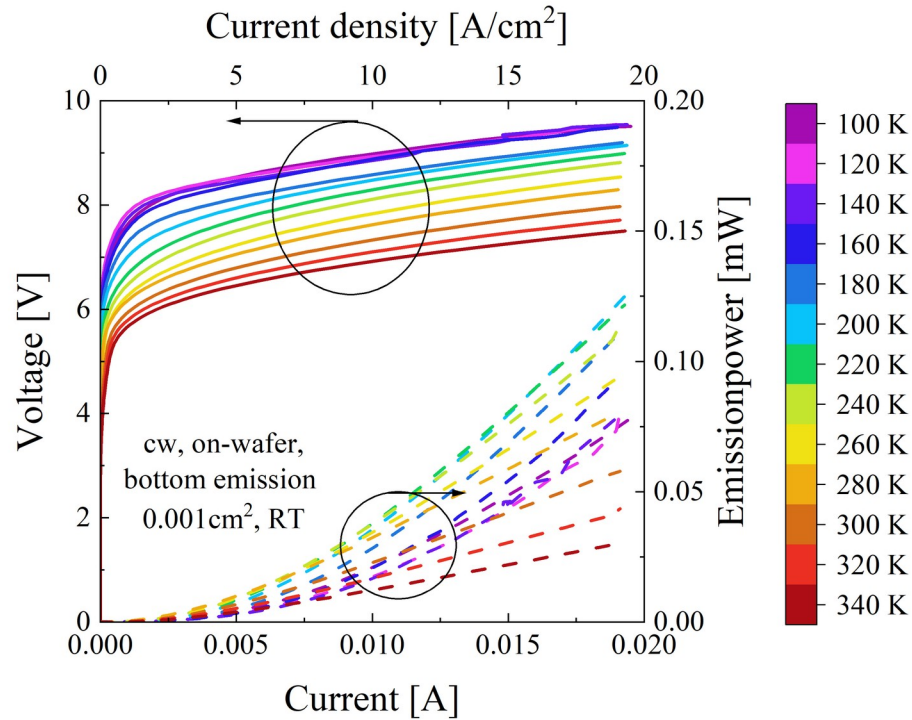


LIV bis 100 mA

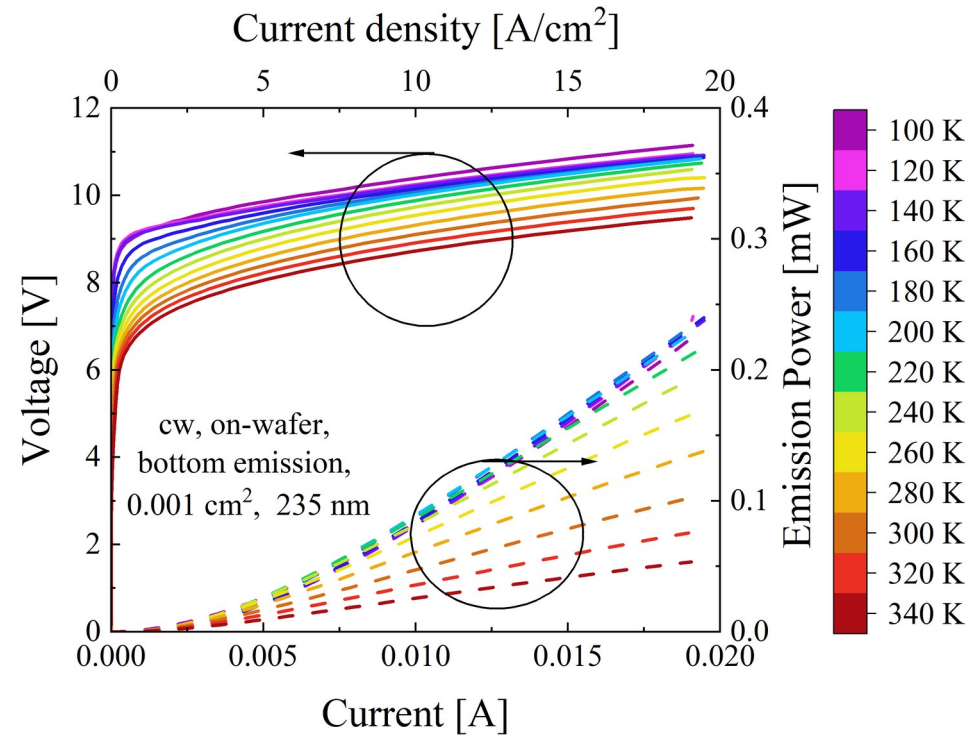


LIV Kurven

900 °C:

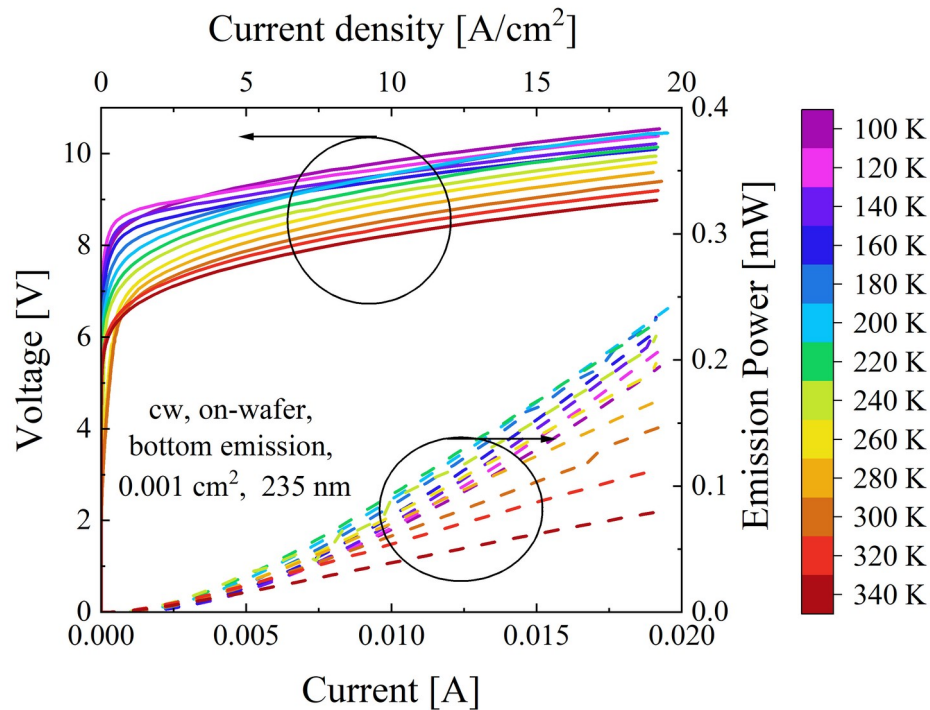


935 °C:

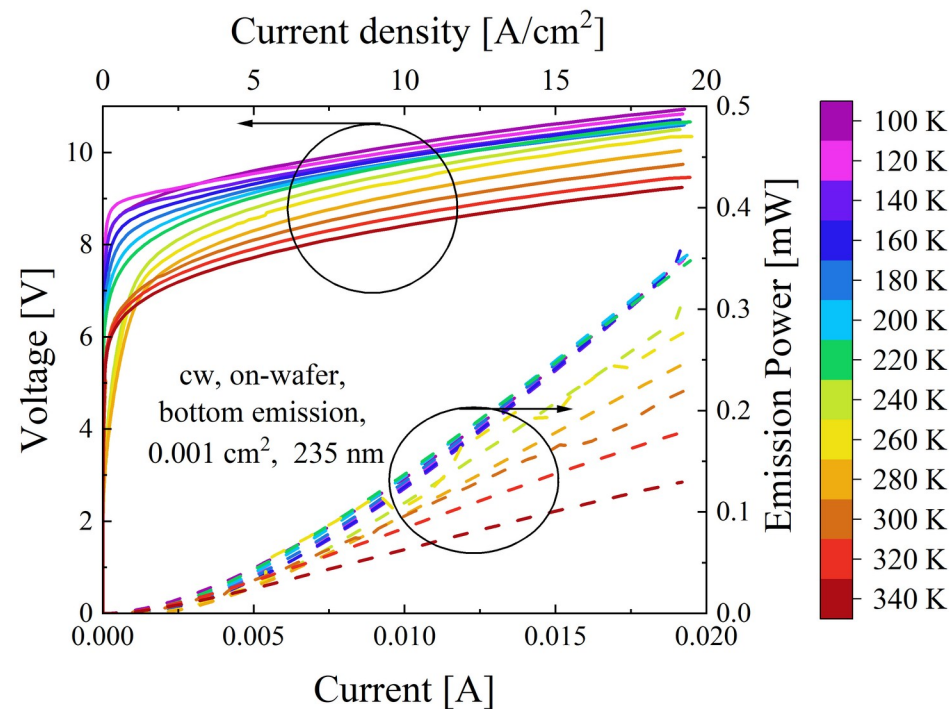


LIV Kurven

970 °C:

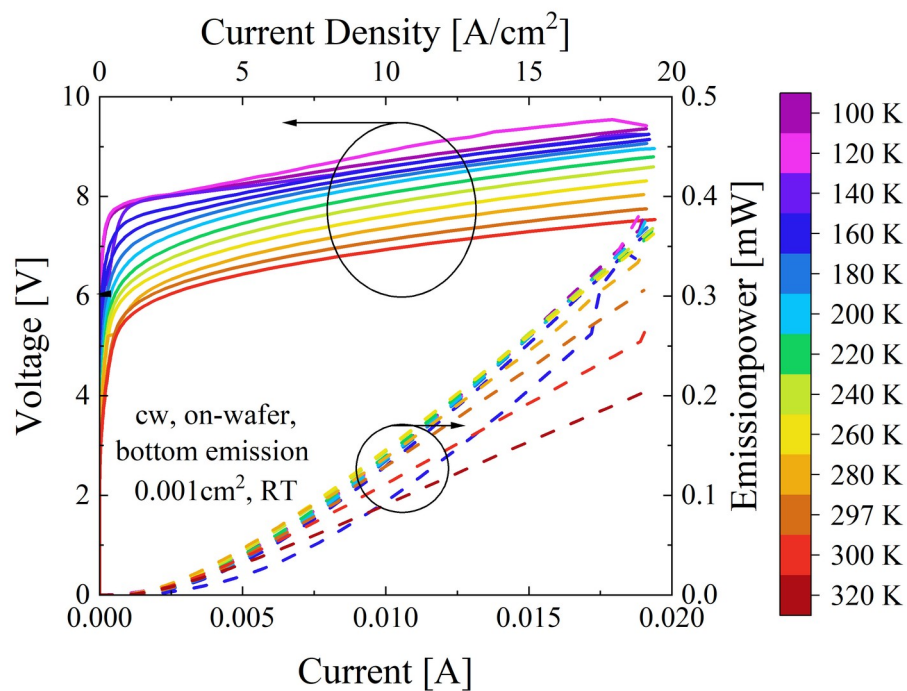


1020 °C:

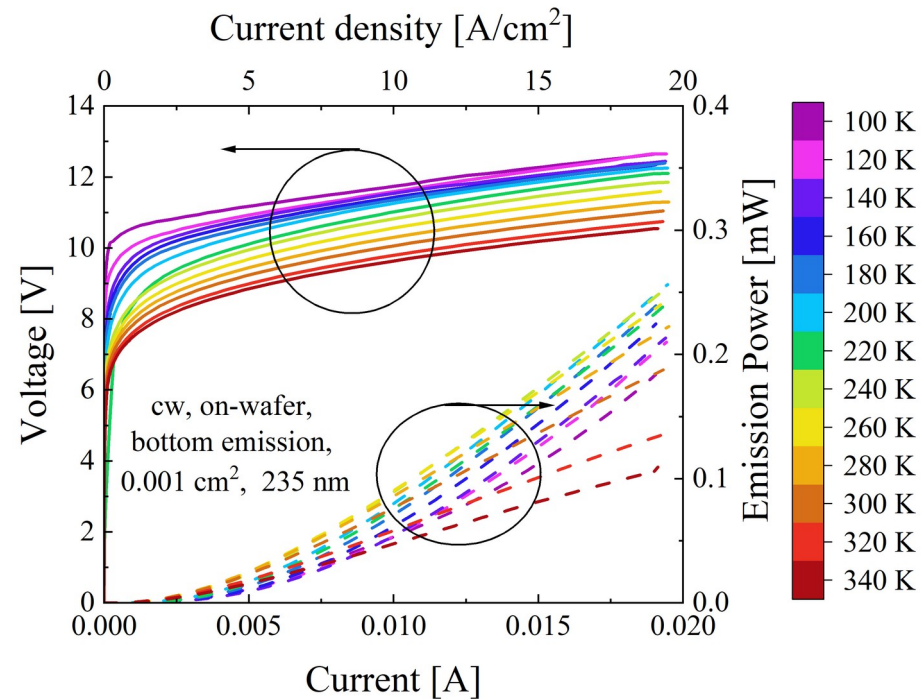


LIV Kurven

1060 °C:

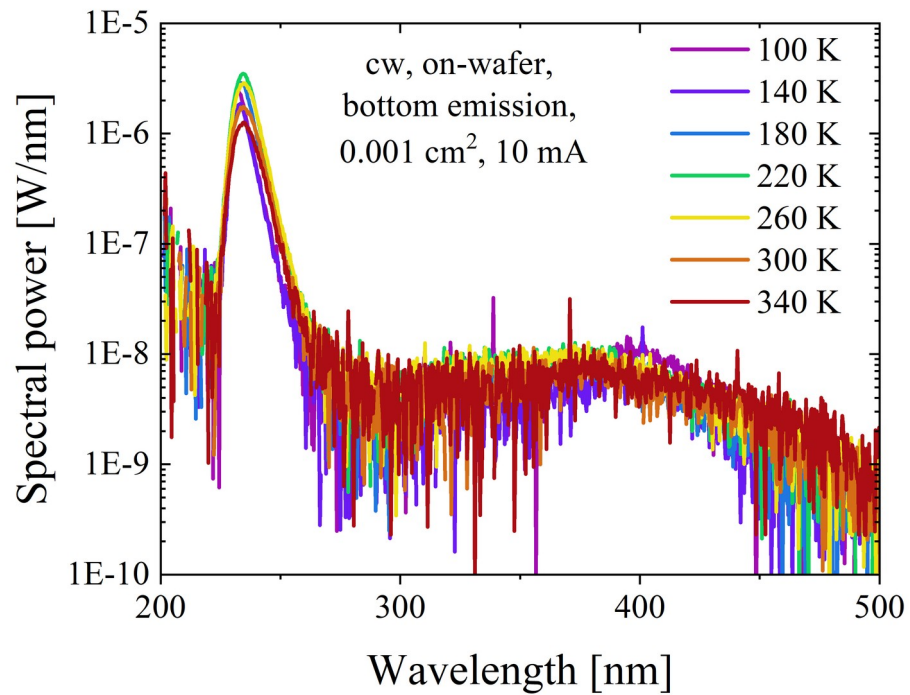


1100 °C:

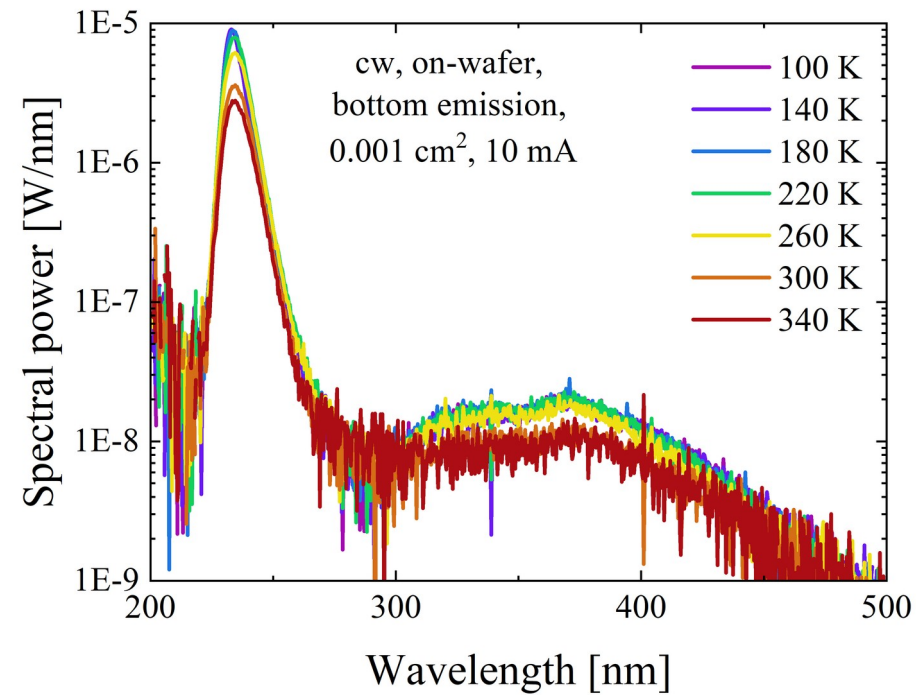


Spektren

900 °C:

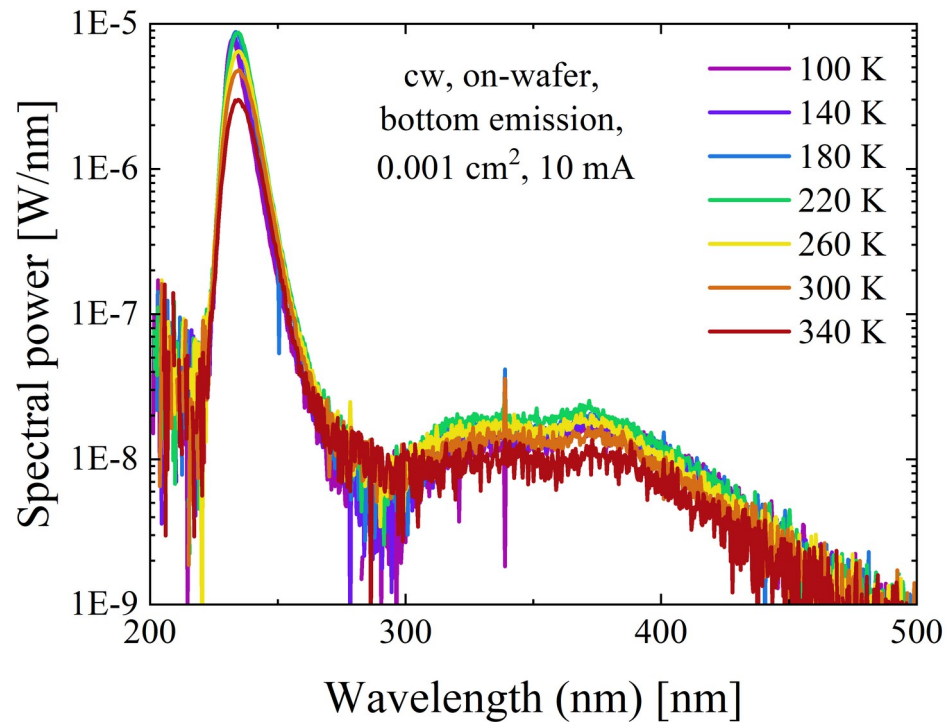


935 °C:

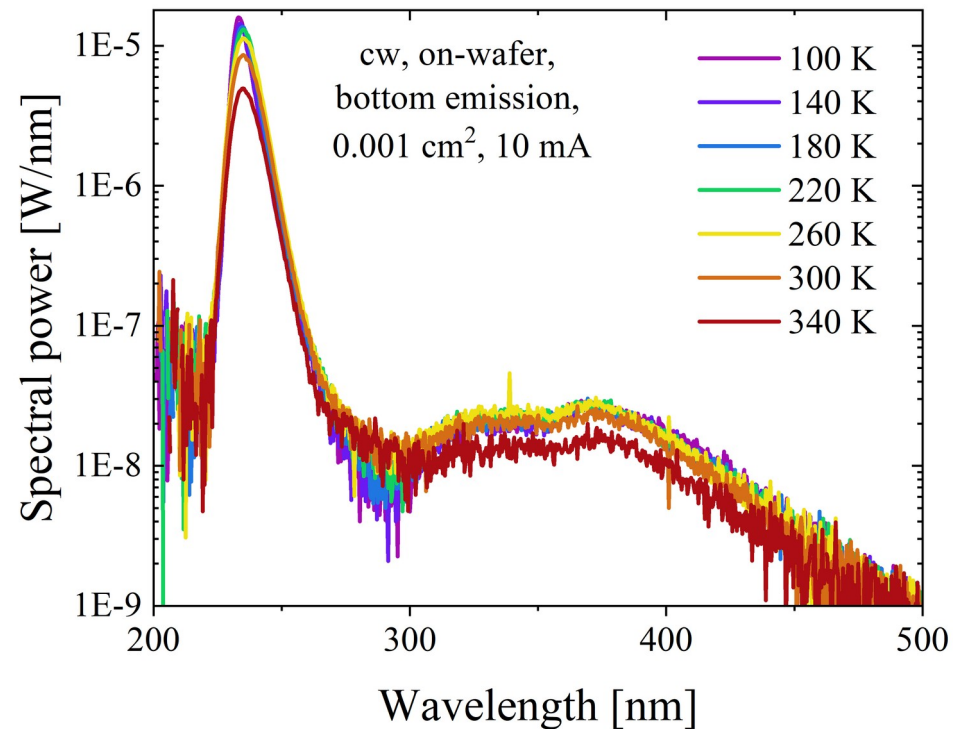


Spektren

970 °C:

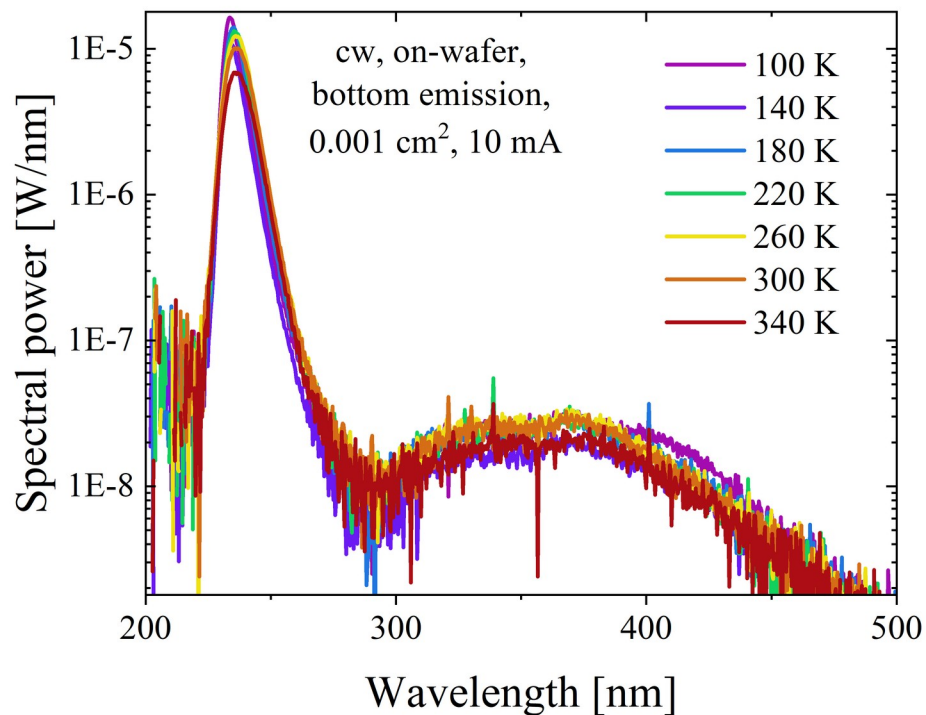


1020 °C:



Spektren

1060 °C:



1100 °C:

